MOLECULAR
METABOLISM

LEAP2 deletion in mice enhances ghrelin's actions as an orexigen and growth hormone secretagogue

Kripa Shankar [1,6], Nathan P. Metzger [1,6], Omprakash Singh [1,6], Bharath K. Mani [1], Sherri Osborne-Lawrence [1], Salil Varshney [1], Deepali Gupta [1], Sean B. Ogden [1], Shota Takemi [1], Corine P. Richard [1], Karabi Nandy [3], Chen Liu [1,2], Jeffrey M. Zigman [1,4,5,]*

ABSTRACT

Objective: The hormone liver-expressed antimicrobial peptide-2 (LEAP2) is a recently identified antagonist and an inverse agonist of the growth hormone secretagogue receptor (GHSR). GHSR's other well-known endogenous ligand, acyl-ghrelin, increases food intake, body weight, and GH secretion and is lowered in obesity but elevated upon fasting. In contrast, LEAP2 reduces acyl-ghrelin-induced food intake and GH secretion and is found elevated in obesity but lowered upon fasting. Thus, the plasma LEAP2/acyl-ghrelin molar ratio could be a key determinant modulating GHSR signaling in response to changes in body mass and feeding status. In particular, LEAP2 may serve to dampen acyl-ghrelin action in the setting of obesity, which is associated with ghrelin resistance. Here, we sought to determine the metabolic effects of genetic LEAP2 deletion.

Methods: We generated the first known LEAP2-KO mouse line. Food intake, GH secretion, and cellular activation (c-fos induction) in different brain regions following s.c. acyl-ghrelin administration in LEAP2-KO mice and wild-type littermates were determined. LEAP2-KO mice and wild-type littermates were submitted to a battery of tests (such as measurements of body weight, food intake, and body composition; indirect calorimetry, determination of locomotor activity, and meal patterning while housed in metabolic cages) over the course of 16 weeks of high-fat diet and/or standard chow feeding. Fat accumulation was assessed in hematoxylin & eosin-stained and oil red O-stained liver sections from these mice.

Results: LEAP2-KO mice were more sensitive to s.c. ghrelin. In particular, acyl-ghrelin acutely stimulated food intake at a dose of 0.5 mg/kg BW in standard chow-fed LEAP2-KO mice while a $2\times$ higher dose was required by wild-type littermates. Also, acyl-ghrelin stimulated food intake at a dose of 1 mg/kg BW in high-fat diet-fed LEAP2-KO mice while not even a $10\times$ higher dose was effective in wild-type littermates. Acyl-ghrelin induced a 90.9% higher plasma GH level and 77.2–119.7% higher numbers of c-fos-immunoreactive cells in the arcuate nucleus and olfactory bulb, respectively, in LEAP2-KO mice than in wild-type littermates. LEAP2 deletion raised body weight (by 15.0%), food intake (by 18.4%), lean mass (by 6.1%), hepatic fat (by 42.1%), and body length (by 1.7%) in females on long-term high-fat diet as compared to wild-type littermates. After only 4 weeks on the high-fat diet, female LEAP2-KO mice exhibited lower O_2 consumption (by 13%), heat production (by 9.5%), and locomotor activity (by 49%) than by wild-type littermates during the first part of the dark period. These genotype-dependent differences were not observed in high-fat diet-exposed males or female and male mice exposed for long term to standard chow diet.

Conclusions: LEAP2 deletion sensitizes lean and obese mice to the acute effects of administered acyl-ghrelin on food intake and GH secretion. LEAP2 deletion increases body weight in females chronically fed a high-fat diet as a result of lowered energy expenditure, reduced locomotor activity, and increased food intake. Furthermore, in female mice, LEAP2 deletion increases body length and exaggerates the hepatic fat accumulation normally associated with chronic high-fat diet feeding.

1. INTRODUCTION

Liver-expressed antimicrobial peptide-2 (LEAP2) is a forty amino-acid-long peptide hormone ligand of the growth hormone secretagogue receptor (GHSR) [1]. Originally isolated in 2003, LEAP2 is expressed predominantly in the liver and small intestine in both mice and humans; the kidney is another major expression site in humans [1–3]. Ge et al. used *in vitro* signaling assays to determine potent and

[1]Center for Hypothalamic Research, Department of Internal Medicine, UT Southwestern Medical Center, Dallas, TX, USA [2]Department of Neuroscience, UT Southwestern Medical Center, Dallas, TX, USA [3]Division of Biostatistics, Department of Population and Data Sciences, UT Southwestern Medical Center, Dallas, TX, USA [4]Division of Endocrinology, Department of Internal Medicine, UT Southwestern Medical Center, Dallas, TX, USA [5]Department of Psychiatry, UT Southwestern Medical Center, Dallas, TX, USA

[6] These authors contributed equally to the manuscript.

*Corresponding author. Center for Hypothalamic Research Department of Internal Medicine UT Southwestern Medical Center, 5323 Harry Hines Blvd., MC 9077 Dallas, TX, 75390-9077, USA. Fax: +1 214 648 5612. E-mail: jeffrey.zigman@utsouthwestern.edu (J.M. Zigman).

selective GHSR antagonist activity for LEAP2 [1]. Corroborating these *in vitro* findings, LEAP2 administration dose-dependently blocked the effects of GHSR's other well-known endogenous ligand, acyl-ghrelin to induce food intake and GH secretion in mice [1]. Viral-mediated LEAP2 overexpression during prolonged caloric restriction phenocopied the life-threatening hypoglycemia described for calorically-restricted mice lacking acyl-ghrelin or with defective ghrelin secretion [4–8]. Furthermore, administration of anti-LEAP2 neutralizing antibodies to 24-h fasted mice raised plasma GH levels, leading the authors of that study to conclude that "blocking endogenous LEAP2 promotes ghrelin-mediated GHSR activation *in vivo*" [1].

Since the initial description of LEAP2 as a GHSR ligand, the physiology of LEAP2 as it relates to the ghrelin system and metabolism has been investigated in several additional studies. For instance, Islam et al. blocked acute food intake as induced by i.c.v. administration of a single acyl-ghrelin bolus to rats by co-administering LEAP2 [9]. A similar effect of LEAP2 on acyl-ghrelin-induced food intake was observed in rats when both were peripherally administered [9]. However, rebound feeding in rats in the first 2 h following a 14 h fast was not impacted by i.c.v.-administered LEAP2 [9]. Also, central LEAP2 administration eliminated the rises in blood glucose and plasma GH levels and the drop in body temperature normally induced in rats acutely by acyl-ghrelin [9]. M'Kadmi et al. reported that although LEAP2 alone and an N-terminal LEAP2 fragment alone did not affect food intake when administered s.c. to mice, they either blocked or blunted food intake induced by acyl-ghrelin [10]. Similar effects were reported by Barrile et al. in C57BL/6J mice centrally administered LEAP2 or a fluorescence-tagged N-terminal LEAP2 fragment [11]. Moreover, Cornejo et al. demonstrated that i.c.v. administration of an N-terminal LEAP2 fragment reduced high-fat diet eating during a binge-like eating protocol in C57BL/6J mice [12].

Notably, whole-cell patch-clamp electrophysiology recordings demonstrated that LEAP2 can reverse acyl-ghrelin-induced membrane depolarization of arcuate hypothalamic neuropeptide Y (NPY) neurons [13]. LEAP2 also can hyperpolarize hypothalamic NPY neurons, while acyl-ghrelin fails to alter hypothalamic NPY neuron membrane potential in brain slices pretreated with an equimolar amount of LEAP2 [13]. LEAP2 also reduces signaling in GHSR-expressing human embryonic kidney 293 (HEK293) cells [10]. These data suggest that LEAP2 acts both as a powerful GHSR antagonist and a GHSR inverse agonist that disables GHSR constitutive activity.

Levels of circulating LEAP2 also have been investigated in several settings since plasma LEAP2 was first shown to fall after a 24 h fast and rise after re-feeding, in a pattern opposite to that of total ghrelin (acyl-ghrelin + desacyl-ghrelin) [1]. Mani et al. showed that plasma LEAP2 increased with body mass, body mass index, body fat, blood glucose, food intake (in subjects with obesity), homeostatic model assessment of insulin resistance (HOMA-IR), serum triglycerides, visceral adiposity, and intrahepatocellular lipid content in C57BL/6N mice and/or human subjects [13]. In contrast, plasma LEAP2 decreased with 24-h fasting, diet-induced weight loss, and weight loss associated with Roux-en-Y gastric bypass or vertical sleeve gastrectomy [13]. These changes were mostly opposite to those of plasma acyl-ghrelin [13]. This translated to an increase in the mean plasma LEAP2: acyl-ghrelin molar ratio in states of nutritional abundance, such as obesity (especially postprandially), and a decrease in the mean plasma LEAP2:acyl-ghrelin molar ratio in states of nutritional deficiency, such as after weight loss or after an acute fast [13]. Ma et al. demonstrated increased circulating LEAP2 and reported increased hepatic LEAP2 content in high-fat diet-fed C57BL/6J mice as compared to standard chow diet-fed mice [14]. Also, plasma LEAP2

was positively correlated with body mass index, HOMA-IR, waist-to-hip ratio, fasting insulin, age, and hepatic fat content in humans [14]. Islam et al. also demonstrated a drop in plasma LEAP2 with fasting and recovery with re-feeding, in a direction opposite to that of plasma ghrelin in rats [9]. Barja-Fernandez et al. revealed a positive correlation between plasma LEAP2 and HOMA-IR in children [15]. In girls, plasma LEAP2 also was positively correlated with body weight, Tanner stage, lean mass, and plasma triglycerides, while in boys, plasma LEAP2 showed a correlation with fat mass and blood glucose [15]. Additionally, plasma LEAP2 was positively correlated with % fat mass in pubertal children but not in prepubertal children [15].

These findings differ from those of Aslanipour et al., in which plasma LEAP2 was negatively correlated with body mass index and HOMA-IR in women with the polycystic ovarian syndrome and body mass index-matched controls [16]. Also, Fittipaldi et al. reported lower plasma LEAP2 in children with overweight/obesity as compared to normal-weight controls [17]. Hagemann et al. documented that plasma LEAP2 was either slightly reduced or unchanged during a mixed-meal tolerance test performed one week or 3 months, respectively, after Roux-en-Y gastric bypass [18]. Plasma LEAP2 showed no correlation with body mass index in a study by Francisco et al. that compared subjects with rheumatoid arthritis to healthy controls, although plasma LEAP2 was higher in subjects with rheumatoid arthritis [19].

Setting aside the findings in the latter four studies, the aforementioned data led to the hypothesis that LEAP2 might offset the actions of acyl-ghrelin and contribute to the state of ghrelin resistance associated with obesity [20–23]. For example, acyl-ghrelin fails to acutely induce food intake in diet-induced obese mice and in obese Agouti mice whether acutely or chronically administered [24–26]. Administered acyl-ghrelin fails to reduce energy expenditure in diet-induced obese mice unlike its clear effect to reduce energy expenditure in mice fed on regular chow [27]. Also, acyl-ghrelin-induced GH release is attenuated in obese human subjects [28]. It remains unknown whether, in the setting of obesity in which many studies demonstrate high plasma LEAP2 and low plasma acyl-ghrelin, LEAP2 antagonizes acyl-ghrelin action, thereby limiting acyl-ghrelin's capacity to further raise food intake and reduce energy expenditure. In the current study, we generated a novel LEAP2-knockout (KO) mouse model to determine the consequences of genetic LEAP2 deletion on several metabolic parameters, with an overall goal to better understand the overall physiological significance of LEAP2 as it relates to metabolism.

2. METHODS AND MATERIALS

2.1. Animal care

Mice were housed at 21.5°C-22.5 °C with a 12-h light–12-h dark cycle and free access to standard chow (2916, Teklad Global 16% Protein Rodent Diet, Envigo, Indianapolis, IN) plus water, unless otherwise noted. Body weights of standard chow-fed mice were determined at the start of each of the metabolic manipulations performed and were found to be equivalent between genotypes. The UT Southwestern Medical Center Institutional Animal Care and Use Committee approved all experiments.

2.2. Generation of LEAP2-KO mice

LEAP2-KO mice were generated using CRISPR/*Cas9* technology via microinjection of *Cas9* mRNA, two short guide RNAs (sgRNAs), and two donor oligonucleotides containing *loxP* sites flanked by homology arms into C57BL/6N zygotes. The *Cas9*-mediated double-strand breaks were directed by guide RNAs designed to bind genomic

sites 612 bp upstream and 280 bp downstream of the LEAP2 coding sequence (upstream *loxP*: 5′AGTTTGAGCTCCTTATAΔGCC-3′; downstream *loxP*: 5′-GCCACTACTACTCCCTAΔTAA-3′; *Cas9* cut site is indicated by Δ). The procedure resulted in four independent mouse lines with the deletion of the entire LEAP2 coding sequence in addition to deletion of about 600 bp upstream and 300 bp downstream of the *Leap2* gene, without insertion of *loxP* sites. Genomic editing in the target locus was confirmed by PCR analysis of tail genomic DNA using primers M808 (5′-TACCTCCTCCCTCGTGTGTC-3′) and M811 (5′-CAGATGGTACACACCAGCCTAA-3′), followed by DNA sequencing to determine the extent of the deletion. The LEAP2-KO cell line designated "LKO3" was chosen for the experiments described here. Figure 1A shows both the WT *Leap2* and the mutant allele with deletion of the LEAP2 coding sequence (LEAP2-KO) that resulted via non-homologous end-joining of the *Cas9*-mediated breaks after deleting the flanked sequence. The LKO3 founder was crossed to C57BL/6N mice and resulting heterozygous progeny were crossed to each other to generate homozygotes, heterozygotes, and WT mice in the expected Mendelian genetic ratio. Genotyping was performed on tail genomic DNA using M808 and M811 together with a third primer, M827 (5′-ACAGACTGTCTATGGTGCTCTA-3′). Homozygotes (LEAP2-KO) and wild-types resulting from crosses of mice heterozygous for the *Leap2-KO* allele were used for the current studies.

2.3. Long-term feeding studies

In one cohort of mice, female and male LEAP2-KO and WT-littermate mice were individually housed starting at 4 weeks of age (1 week after weaning) and fed a standard chow diet *ad lib* for 16 weeks. Body-weight and food intake were measured weekly. Body composition analysis was performed using an EchoMRI-100 apparatus (EchoMRI LLC, Houston, TX, USA) in an *ad lib*-fed state at 4 (in females only), 8, and 16 weeks-of-age and in a 24 h-fasted condition at 12 and 20 weeks of age. *Ad lib*-fed plasma LEAP2, plasma acyl-ghrelin, and blood glucose were determined at 16 weeks of age; 24 h−fasted plasma LEAP2, plasma acyl-ghrelin, and blood glucose were determined at 20 weeks of age. Blood samples were collected by quick superficial temporal vein bleed.

In another cohort of mice, female and male LEAP2-KO and WT-littermate mice were individually housed starting at 4 weeks-of-age and fed a Western-type high-fat diet (Envigo Teklad TD88137; with an energy density of 4.5 kcal/g, of which 42% of kcal was derived from fat) *ad lib* for 16 weeks. Measurements on the high-fat diet-fed mice were similar to those described above.

Following these 16-week long-term feeding studies, the female mice were maintained on the same standard chow or high-fat diet for another 2−4 weeks, at which time a subset of the mice (now aged 22−24 weeks) were sacrificed and their tissues collected for liver
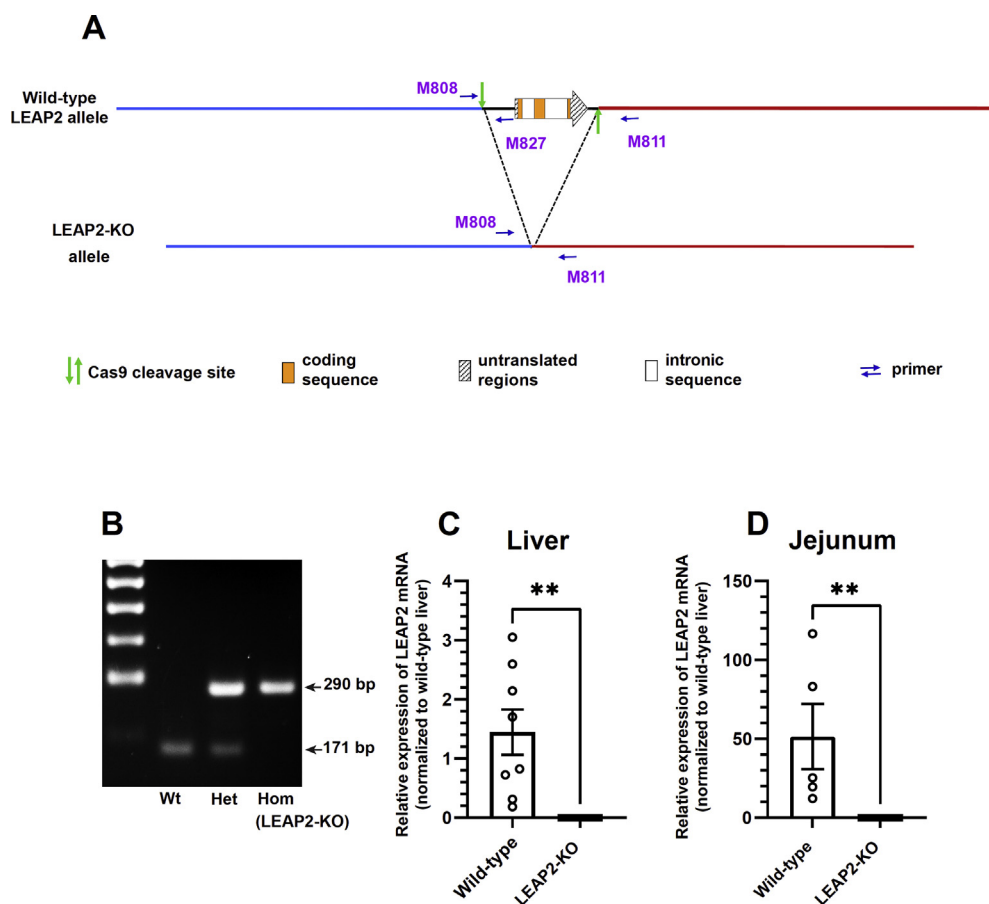

Figure 1: Generation and validation of LEAP2-KO mice. **(A)** Schematic diagrams show the CRISPR-Cas9 strategy to delete the LEAP2 coding region. **(B)** PCR analysis of genomic DNA obtained by tail biopsies of representative mice derived from crosses of mice heterozygous for the *Leap2-KO* allele, demonstrating the identification of mice with two copies of the wild-type *Leap2* allele (WT), mice homozygous for the *Leap2-KO* allele (HOM), and heterozygotes (HET). mRNA expression of *Leap2* in **(C)** liver and **(D)** jejunum. n = 6−9 per each genotype. Data are presented as mean ± s.e.m. Data were analyzed by Student's t-test. Statistically significant differences are indicated by asterisks: *$P < 0.05$; **$P < 0.01$ and ***$P < 0.001$.

histology and quantitative reverse-transcriptase PCR assessments (see subsections 2.4, 2.8 below for more details). Separate subsets of the female mice were anesthetized with chloral hydrate (500 mg/kg BW i.p.) at 22-25 weeks-of-age (those on standard chow) or at 23-24 weeks-of-age (those on a high-fat diet), at which time body (nose-to-anus) length was determined using a protractor. The male mice enrolled in the 16-week long-term feeding studies also were maintained on the same standard chow or high-fat diets, this time for another 2—6 weeks. At ages 21—23 weeks, the standard chow-fed male mice underwent a fast/re-feeding protocol (see section 2.5 below for details). One week later (at ages 22—24 weeks), the standard chow-fed male mice underwent an administered ghrelin-induced food intake study (see below for details; 2.6). A subset of the standard chow-fed male mice underwent an acyl-ghrelin-induced c-fos induction study at 25—26 weeks of age (see below for details; 2.7). At age 22—23 weeks, a subset of the high-fat diet-fed male mice underwent an administered ghrelin-induced food intake study (see below for details; 2.6). One week later (at ages 23—24 weeks), all the available high-fat diet-fed male mice underwent a fast/re-feeding protocol (see below for details; 2.5).

Notably, the above-mentioned results and the corresponding schematic diagrams of the general experimental approach (Figure S1) reveal that all of the experimental paradigms were not performed on both female and male mice and in both high-fat diet and standard chow conditions. It was not logistically possible (without requiring different sets of mice) or financially sound to assess all parameters in every animal.

2.4. Liver histology

Two-four weeks after completion of the long-term standard chow and high-fat diet feeding studies, a subset of the female mice (aged 22—24 weeks of age) that had been maintained on their same diets were anesthetized with chloral hydrate (500 mg/kg BW i.p.) and euthanized by quick decapitation. A portion of the right side of the liver was collected and submerged in 10% formalin solution at 4 °C overnight, followed by immersion in 25% sucrose in diethylpyrocarbonate (DEPC)-treated PBS, pH 7.0 at 4 °C overnight. Subsequently, the formalin-fixed liver portions were placed in OCT solution, frozen on dry ice, sectioned at a thickness of 10 μm using a cryostat (CM3050S, Leica Biosystems, Buffalo Grove, IL), and placed on SuperFrost slides (Cat # 12-500-15, Thermo Fisher Scientific, Pittsburgh, PA). Multiple series of slide-mounted liver sections each separated by at least 200 μm were prepared and stored at −20 °C until further processing. One series was stained using a standard hematoxylin & eosin protocol. Another series underwent oil red O staining, which involved a brief rinse in tap water, submersion in working oil red O solution for 15 min, a wash in water, staining with hematoxylin (Cat # 72,804, Thermo Scientific) for 3 min, a final wash in water for 5 min, and coverslipping (Cat # 12-545-M, Fisher Scientific) with aqueous mounting media (Glycerol, Sigma Aldrich, St. Louis, MO). Images of the stained sections were taken using the 10× objective of a Leica DM6 B digital research microscope (Leica Microsystems Gmbh, Wetzlar, Germany) equipped with a Leica DFC 9000 GT digital microscopy camera and LAS X software. Photomicrographs were equally adjusted for the size in Adobe Photoshop 22.3.0 software (Adobe Systems, San Jose, CA). All parameters of the images such as size, brightness, contrast, and sharpness were kept constant during quantification. Images of oil red O-stained sections were first subjectively analyzed in a blinded fashion by rating the amount of oil red O present (a surrogate of triglyceride content). Next, the percentage of each oil red O-positive (oil red O % +ve area) section, the total number of oil red O-stained lipid droplets, and the number of oil red O lipid droplets were determined for each of 2—3 representative sections from each mouse, using Image J software (NIH, Bethesda, MD).

2.5. Fast/re-feeding

One-three weeks following the long-term standard chow feeding studies (in male mice aged 21—23 weeks) and three-four weeks following long-term high-fat diet feeding studies (in male mice aged 23—24 weeks), during which time the mice were maintained on the same diets, the mice were fasted for 24 h, starting at 9 a.m. The next day at 9 a.m., pre-weighed pellets of either standard chow or high-fat diet were provided at the bottom of the cages. Food intake was determined at 1, 2, 4, and 24 h.

2.6. Administered acyl-ghrelin-induced food intake and growth hormone secretion

Two-four weeks following the long-term feeding studies, during which time the mice were maintained on their same diets, all available standard chow-fed male mice (22—24 weeks of age) and a subset of the high-fat diet-fed male mice (22—23 weeks of age) were handled for 3 days to acclimatize them. On the 4th day, access to food was restricted for 2 h prior to an 11:00 a.m. s.c. injection of saline and re-introduced immediately after the injection. In the standard chow-fed mice, on the 5th —8th days, access to food was restricted each morning for 2 h prior to an 11:00 a.m. s.c. injection of increasing doses of rat acyl-ghrelin (SP-GHRL-1; Innovagen, Lund, Sweden; 0.1, 0.25, 0.5, or 1.0 mg/kg BW). A single pre-weighed standard chow pellet was re-introduced on the cage floors immediately after the injection. In the high-fat diet-fed mice, on the 5th—6th days, access to food was restricted each morning for 2 h prior to an 11:00 a.m. s.c. injection of increasing doses of rat acyl-ghrelin (1.0 or 10 mg/kg BW). A single pre-weighed high-fat diet pellet was re-introduced on the cage floors immediately after the injection. The amounts eaten over the subsequent 1 h and 2 h after acyl-ghrelin treatment were determined.

In a separate cohort of 10- to 12-week-old standard chow-fed male mice (not taken from the long-term feeding studies or other studies), acyl-ghrelin-induced GH secretion was assessed. Fifteen minutes after anesthesia with pentobarbital (50 mg/kg BW, i.p.), rat acyl-ghrelin (0.1 mg/kg i.p.) was injected. Blood was sampled from tail snips just prior to and 15 min after administration of acyl-ghrelin to determine plasma GH levels.

2.7. Immunohistochemistry for c-fos

A subset of wild-type and LEAP2-KO male mice from the long-term standard chow feeding study that had been maintained on standard chow for another 5—6 weeks after the end of the study were handled for 3 days. On day 4, they were administered either saline or acyl-ghrelin (0.5 mg/Kg BW s.c.) and kept food-restricted for the following 2 h. Afterward, the mice were deeply anesthetized at ages 25—26 weeks with an i.p. injection of chloral hydrate (500 mg/Kg BW) and perfused transcardially with diethyl pyrocarbonate (DEPC)-treated 0.9% phosphate-buffered saline (PBS) followed by 10% neutral buffered formalin, as described previously [29]. Brains were dissected out, postfixed in the same fixative overnight at 4 °C, and then cryoprotected by immersing in 25% sucrose solution in DEPC-treated PBS overnight at 4 °C. After embedding in Tissue-Tek OCT compound, serial 25-μm thick coronal sections extending from the olfactory bulb to the cervical spinal cord were obtained using a cryostat, immersed in anti-freeze solution, separated into five equal series, and then stored at −20 °C until further processing. One series from each saline and acyl-ghrelin-administered WT and LEAP2-KO mice (n = 5) was processed for c-fos

immunofluorescence as previously described, with minor modifications [30]. Sections were rinsed in PBS, immersed in 0.5% Triton X-100 solution in PBS for 30 min, and blocked in 3% normal donkey serum (Cat # 017-000-121, Jackson ImmunoResearch Laboratories, Inc., West Grove, PA) in PBS for 2 h. Sections were incubated in diluted rabbit anti-c-fos antibody (Cat # PC38, Calbiochem/Oncogene, Temecula, CA; dilution 1:20,000) for 24 h at room temperature. After washing in PBS, the sections were incubated in Alexa Fluor® 488 donkey anti-rabbit IgG (Cat # A21206, Invitrogen, Carlsbad, CA; dilution 1:500) for 2 h at room temperature, and following additional washing in PBS, sections were mounted onto SuperFrost slides, dried overnight and cover slipped with Vectashield mounting media with 4′,6-diamidino-2-phenylindole (DAPI) [Cat # H-1200, Vector Labs, Burlingame, CA]. Stained brain sections of two different levels of the arcuate nucleus [ARC; Bregma −1.82 and −2.06 mm] and one level of the olfactory bulb [OB; Bregma 4.28 mm] were imaged using 10× and 20× objectives of a Leica DM6 B digital research microscope equipped with Leica DFC 9000 GT digital microscopy camera, and LAS X software. Photomicrographs were equally adjusted for the size and brightness in Adobe Photoshop 22.3.0 software (Adobe Systems, San Jose, CA). All parameters were kept constant during quantification. Cells showing clear, round c-fos-immunoreactive nuclei were manually counted with the assistance of the Adobe Photoshop counting tool bilaterally at each of the two levels of the ARC and added together to obtain a value for each mouse. Cells with c-fos immunoreactivity were manually counted unilaterally in the one level of the OB for each mouse.

2.8. Quantitative reverse transcriptase-PCR

A subset of the female mice from the long-term standard chow diet feeding study was maintained on standard chow for another 2—4 weeks, at which time the mice were deeply anesthetized with i.p. injection of chloral hydrate (500 mg/kg) and then euthanized by cervical dislocation. Liver and jejunum were immediately collected into RNAlater (Invitrogen) media, stored at 4 °C overnight or up to one week, then RNAlater was removed and the tissues were either immediately processed to isolate RNA or frozen at −20 °C until further processing. Total RNA was isolated using the guanidium thiocyanate-phenol-chloroform extraction method with the addition of RNA STAT-60 (AMSBIO, Cambridge, MA). The isolated RNA was quantified using a Nanodrop spectrophotometer (Thermo Fisher Scientific). Total RNA (83 ng per gene) was treated with ribonuclease-free deoxyribonuclease (Roche, IN), and complementary DNA was synthesized by reverse transcription using SuperScript III (Invitrogen).

Quantitative PCR was performed using the QuantSTUDIO 5 Real-Time PCR System (Applied Biosystems by Thermo Fisher Scientific, Foster City, CA). The mRNA levels are represented relative to the invariant control gene, 18s (TaqMan Gene Expression Assay Mm04277571_s1), and determined using the comparative threshold cycle (ΔΔCt) method. The following primers were used to detect LEAP2 mRNA using SYBR green technology: 79F (5′-GCTGCTGGGTCAGGTCAATAG-3′) and 139R (5′-CCGGGATCTCTTTGCTGAAC-3′). Data are presented relative to the expression of the gene in the livers of wild-type control mice.

2.9. Indirect calorimetry, locomotor activity, and meal pattern analyses

Eight-week-old female mice maintained on a high-fat diet for 4 weeks (starting at 4 weeks of age) were used for indirect calorimetry studies (LabMaster Calorimetry System, TSE Systems; Chesterfield, MO). For these studies, the room temperature was maintained at 22 °C with a 12-h light/dark cycle, and the mice had ad libitum access to high-fat diet and water. First, the mice were placed in a set of cages similar to those used for indirect calorimetry, for an initial 5-d acclimation period. The mice were then transferred to the metabolic chambers, where they were allowed to acclimate for two days. O_2 consumption, CO_2 production, respiratory exchange ratio (RER), and heat production were determined over the subsequent two days for two complete sets of light and dark cycles. During this time, ambulatory activity and rearing activity were monitored with infrared beams. In addition, meal patterns were determined temporally by integrating data from weighing sensors fixed at the top of the cage; the food containers were suspended from these sensors into the sealed cage environment. Meals were defined by a minimum food intake of 0.02 g and at least 10 min between feeding bout events. Notably, the feeding data do not account for potential spillage from the food hoppers. The data were analyzed in three different ways: the first 5 h of the dark-cycle (when the wild-type mice were most active) + the (corresponding) first 5 h of the light-cycle, the total dark-cycle + the total light-cycle, and the total 24-h period.

2.10. Blood collection and determination of plasma hormone levels

Blood samples were collected from quick superficial temporal vein bleed or tail nicks as specified into ethylene diamine tetraacetic acid (EDTA)-coated microtubes kept on ice. The collection tubes contained either the protease inhibitors p-hydroxymercuribenzoic acid (Sigma Aldrich; final concentration 1 mM; for ghrelin measurement) or aprotinin (Sigma Aldrich; final concentration 250 KIU/mL; for LEAP2 measurement) or no additional protease inhibitor (for GH measurements). The samples were immediately centrifuged at 4 °C at 1,500 g for 15 min. For acyl-ghrelin stabilization, HCl was added (1:10) to the p-hydroxymercuribenzoic acid-treated plasma to achieve a final concentration of 0.1 N. Processed samples were stored at −80 °C in small aliquots until further analysis of plasma hormone levels.

ELISA kits were used for acyl-ghrelin (Millipore-Merck, Burlington, MA), GH (Millipore-Merck), and LEAP2 [#EK-075-40; (Human)/LEAP-2 (37—76) (Mouse) EIA Kit; Phoenix Pharmaceuticals, Inc., Burlingame, CA]. According to the manufacturer, the LEAP2 ELISA kit's lower limit of detection = 0.36 ng/mL and its linear range of detection = 0.36ng/mL-6.5 ng/mL. We used 1:4 dilutions of plasma for the LEAP2 assays. Notably, although we previously validated the specificity of this LEAP2 assay kit [13], it is unlikely that the kit's sensitivity in detecting only LEAP2 in plasma was ever tested since a LEAP2-KO mouse line was not previously available. Thus, it is unlikely that the manufacturer of the kit could fully assess whether the LEAP2 antibody used in the kit might bind to an antigen other than LEAP2 in the plasma. Calorimetric assays were performed using a BioTek PowerWave XS Microplate spectrophotometer (BioTek, Winooski, VT) using BioTek KC4 junior software.

2.11. Statistics

Data are presented as mean ± s.e.m. and analyzed by student's t-test or two-way ANOVA, as indicated in the Figure legends. Sidak post hoc testing was used to further investigate differences if significant ANOVA effects were found. All data were analyzed using GraphPad Prism version 9.0.2. Data with significant unequal variance were log-transformed prior to performing analyses. Outliers, if any, were removed using the robust regression and outlier removal (ROUT) test. ns represents no statistical significance. P values less than 0.05 were considered statistically significant, and P values ≥ 0.05 and <0.1 were considered evidence of a statistical trend.

For the c-fos studies, while we did not formally carry out a power analysis to estimate our sample size, we used Tan et al. [31] to guide our choice. Tan et al. [31] used a sample size of four per group and found a significant effect of AgRP neuron ablation on ghrelin-induced

c-fos induction in one level of the ARC. Here, we used a sample size of five per group, for a total of 20, in our c-fos analyses, and examined two levels of the ARC and separately, one level of the OB. In order to get an initial estimate of post hoc power, we calculated partial eta squared for each test and associated power based on these observed effect sizes using SAS® software version 9.4 (SAS, Cary, NC).

3. RESULTS

3.1. Generation and validation of LEAP2-KO mice

We generated a novel line of LEAP2-KO mice by utilizing CRISPR/ *Cas9* technology. As depicted in Figure 1A, the LEAP2-KO line resulted from *Cas9*-mediated breaks flanking the *Leap2* coding sequence followed by non-homologous end joining of the *Cas9*-mediated breaks and deletion of the intervening *Leap2* coding sequence. The extent of the targeted deletion (from 655 bp upstream of the *Leap2* start codon to 271 bp downstream of the *Leap2* stop codon, or rather, 1,616 bp) was confirmed by PCR analysis of tail (genomic) DNA using primers M808 and M811 (Figure 1A and B), followed by DNA sequencing. The LEAP2-KO founder was crossed to C57BL/6N mice to generate heterozygous progeny, which were crossed to each other to generate the expected ratio of wild-type mice, mice heterozygous for the *Leap2-KO* allele, and mice homozygous for the *Leap2-KO* allele (LEAP2-KO mice). To validate the LEAP2-KO mice, *Leap2* mRNA expression was quantified in the livers and jejunum of representative wild-type and LEAP2-KO littermates. *Leap2* mRNA expression, which was on average 3,460% higher in wild-type jejunum than wild-type livers, was undetectable in LEAP2-KO mice in both these tissues (Figure 1C and D).

3.2. LEAP2 deletion augments administered acyl-ghrelin-induced food intake

As discussed above, acyl-ghrelin possesses well-characterized, potent orexigenic activity when administered to lean mice, although its potency as an orexigen is markedly reduced or is absent when administered to diet-induced obese mice. Previous work demonstrating actions of LEAP2 to block acyl-ghrelin action suggests that LEAP2 deletion might have the opposite effect, rather it might enhance acyl-ghrelin actions. Such might even be more evident in the setting of diet-induced obesity, in which plasma LEAP2 levels are higher than usual in wild-type mice. To test these predictions, we administered acyl-ghrelin to individually housed 22-24 week-old male wild-type and LEAP2-KO littermates which had been raised on a standard chow diet. The mice, which did not exhibit genotype-dependent body weight differences (see 3.6 below), were exposed daily to increasing single doses of acyl-ghrelin (from 0 up to 1 mg/Kg BW s.c.), and food intake was determined after 1 h (Figure 2A and B) and 2 h (Figure 2C and D). Wild-type mice exhibited statistically significant increases in 1 h and 2 h food intake over those observed upon saline administration (181% increase at 1 h and 143% increase at 2 h) only following the 1 mg/Kg BW dose of acyl-ghrelin; 0.10, 0.25, and 0.5 mg/Kg BW doses of acyl-ghrelin did not have statistically significant effects on 1 h or 2 h food intake (Figure 2A—D). In contrast, statistically significant increases in 1 h and 2 h food intake over those observed upon saline administration were exhibited in LEAP2-KO mice receiving as low as 0.5 mg/Kg BW acyl-ghrelin in addition to the 1.0 mg/Kg BW dose (0.5 mg/Kg BW acyl-ghrelin: 186% increase at 1 h and 136% increase at 2 h; 1.0 mg/Kg BW acyl-ghrelin: 383% increase at 1 h and 289% increase at 2 h; Figure 2A—D).

This protocol was repeated in individually-housed 22-23 week-old male wild-type and LEAP2-KO littermates raised on a 42% Western-style high-fat diet. Acyl-ghrelin doses ranging from 0 up to 10 mg/ Kg BW s.c. were used in consideration of the ghrelin resistance known to be associated with diet-induced obesity [23,24,32]. Of note, previously, we demonstrated in 10—11 week-old male mice that doses of acyl-ghrelin in the 0.1—0.25 mg/Kg BW range acutely raised plasma acyl-ghrelin to levels approaching those induced physiologically by a 16-hour fast, a 24-hour fast, or a 10-day chronic stress protocol [33]. Plasma acyl-ghrelin levels resulting from s.c. administered doses of acyl-ghrelin in the 1.0 and 2.0 mg/Kg BW range were much higher [33]. Here, no genotype-dependent body weight differences were observed in these high-fat diet-fed male mice (see section 3.7 below). Supporting a state of ghrelin resistance, the diet-induced obese wild-type mice failed to exhibit a statistically significant increase in food intake at 1 h (Figure 2E and F) or 2 h (Figure 2G and H) in response to 1 mg/Kg BW or 10 mg/Kg BW acyl-ghrelin s.c. In contrast, food intake was stimulated by both of those acyl-ghrelin doses in the high-fat diet-fed LEAP2-KO mice. The 1 mg/Kg BW acyl-ghrelin dose increased 1 h food intake and 2 h food intake in the LEAP2-KO by 464% and 397%, respectively over those in saline-treated mice (Figure 2E—H).

3.3. LEAP2 deletion augments administered acyl-ghrelin-induced growth hormone secretion

Several lines of evidence suggest that endogenous LEAP2 also influences GH secretion. Not only does LEAP2 administration dose-dependently block the effects of administered acyl-ghrelin to induce GH secretion in mice, but also anti-LEAP2 neutralizing antibodies boost fasting-induced GH increases [1]. Additionally, humans and mice with a GHSR mutation that reduces GHSR constitutive activity results in a short stature phenotype and reduced GH secretion [34,35]. GHSR-null mice as well as homozygous GHSR-IRES-Cre mice (which exhibit a near-complete absence of *Ghsr* mRNA) exhibit slight reductions in body lengths as compared to wild-type littermates [36,37]. Thus, we next investigated the effects of LEAP2 deletion on GH secretion in response to administered acyl-ghrelin. A cohort of 10—12 week old male wild-type and LEAP2-KO littermates maintained on standard chow-diet were anesthetized with pentobarbital, then blood was collected to determine plasma GH levels before and 15 min after an administered dose of acyl-ghrelin (0.1 mg/Kg BW i.p.). Although acyl-ghrelin induced GH secretion in both genotypes, the % increase in plasma GH was significantly greater in LEAP2-KO mice compared to wild-type littermates (wild-types: 368% increase vs. LEAP2-KO mice: 995% increase; Figure 2I).

3.4. Administered ghrelin induced c-fos activation is enhanced by LEAP2 deletion

Many of ghrelin's physiological actions occur via activation of one or more neuronal populations within the central nervous system. Indeed, s.c. acyl-ghrelin induces c-fos (a marker of cellular activation) in the hypothalamic arcuate nucleus (ARC), the paraventricular hypothalamic nucleus, and the dorsal vagal complex [38,39]. Also, previous work demonstrated that i.c.v. administration of LEAP2 suppresses both i.p. acyl-ghrelin-induced c-fos expression in the ARC and i.c.v. acyl-ghrelin-induced c-fos in the ARC and dorsomedial hypothalamic nucleus, while alone, i.c.v. LEAP2 did not affect c-fos in those regions [9]. Here, we assessed whether LEAP2 deletion also enhances the induction of brain c-fos in response to administered acyl-ghrelin. For these studies, the same dose of acyl-ghrelin (0.5 mg/Kg BW s.c.) that increased 1 h and 2 h food intake in standard chow-fed LEAP2-KO mice but not in wild-type littermates (Figure 2A—B), or saline, was administered to a cohort of 25—26 week-old male LEAP2-KO and wild-type littermates. Following the acyl-ghrelin or saline injections,
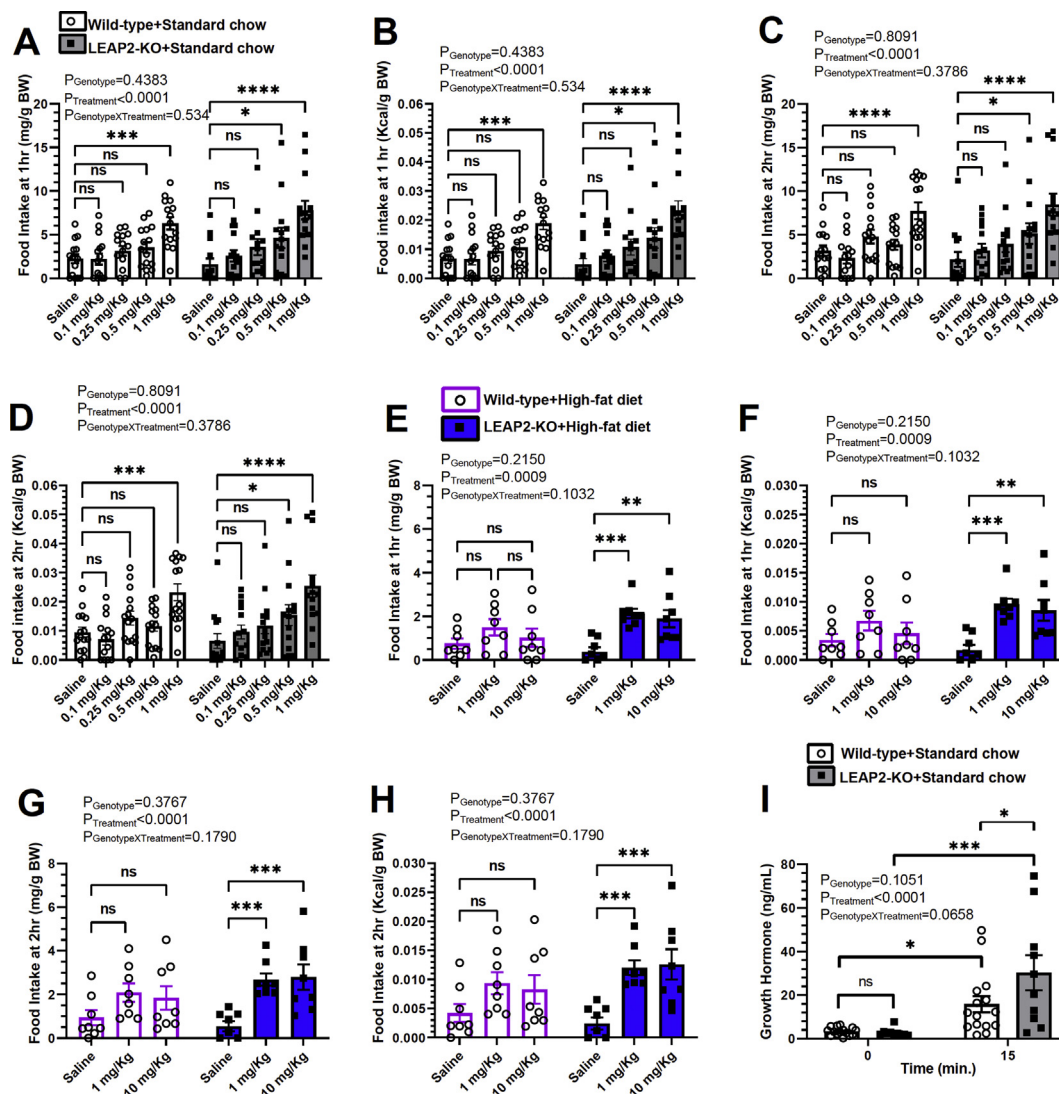
Figure 2: Effect of LEAP2 deletion on acyl-ghrelin-induced food intake and GH secretion. Food intake in long-term standard chow-fed mice measured at (**A, B**) 1 h and (**C, D**) 2 h after saline or acyl-ghrelin (0.1, 0.25, 0.5, and 1 mg/kg BW, s.c.) injection. n = 14—15. Food intake in long-term high-fat diet-fed mice measured at (**E, F**) 1 h and (**G, H**) 2 h after saline or acyl-ghrelin (1 and 10 mg/kg BW, s.c.) injection. n = 8. (**I**) Plasma GH was measured at baseline and 15 min after acyl-ghrelin (0.1 mg/kg BW, i.p.) injection. n = 10—15. Data are presented as mean ± s.e.m. Data were analyzed by two-way repeated-measures ANOVA. Statistically significant differences are indicated by asterisks: $*P < 0.05$; $**P < 0.01$, $***P < 0.001$, $****P < 0.0001$.

the mice were restricted from access to the standard chow diet on which they previously had been maintained. Induction of c-fos was assessed by immunohistochemistry in sections of brains (extending rostro-caudally from the olfactory bulbs to just beyond the dorsal vagal complex) that were taken from the mice 2 h after the acyl-ghrelin or saline injections. In wild-type mice, acyl-ghrelin increased c-fos-immunoreactivity in two brain regions: the ARC and the olfactory bulb (OB) (Figure 3A, C, E, G, I, K, M, N). Within the OB, most of the c-fos-immunoreactivity remained localized to the granular cell (GrO), inner plexiform (IPl), and mitral cell (Mi) layers.

For our objective assessments of c-fos induction, we derived an initial estimate of post hoc power by calculating partial eta squared for each test and associating power based on these observed effect sizes. In particular, for the ARC, the observed partial eta squared ranged from 0.26 to 0.80 with corresponding power between 0.70 and 1.00. For the OB, the observed partial eta squared ranged from 0.37 to 0.78 with

corresponding power between 0.90 and 1.00. Notably, a significantly greater number of c-fos-immunoreactive cells was observed following acyl-ghrelin administration in both the ARC and the OB of LEAP2-KO mice as compared to wild-type mice (Figure 3B, D, F, H, J, L—N). Specifically, there were 77.2% more c-fos-immunoreactive ARC cells following acyl-ghrelin in LEAP2-KO mice than in wild-type mice (Figure 3M). There were 119.7% more c-fos-immunoreactive OB cells following acyl-ghrelin in LEAP2-KO mice than in wild-type mice (Figure 3N). Unlike previous studies in which 2.0 mg/Kg BW acyl-ghrelin administered s.c. to ~ 6-9 week-old wild-type mice induced c-fos in the paraventricular hypothalamic nucleus and dorsal vagal complex in addition to the ARC [38,39], here, 25- to 26-week-old mice administered 0.5 mg/kg BW acyl-ghrelin s.c. exhibited only scattered c-fos-immunoreactive cells in the paraventricular hypothalamic nucleus and dorsal vagal complex in addition to the ARC; there were no obvious increases in c-fos immunoreactivity in those regions
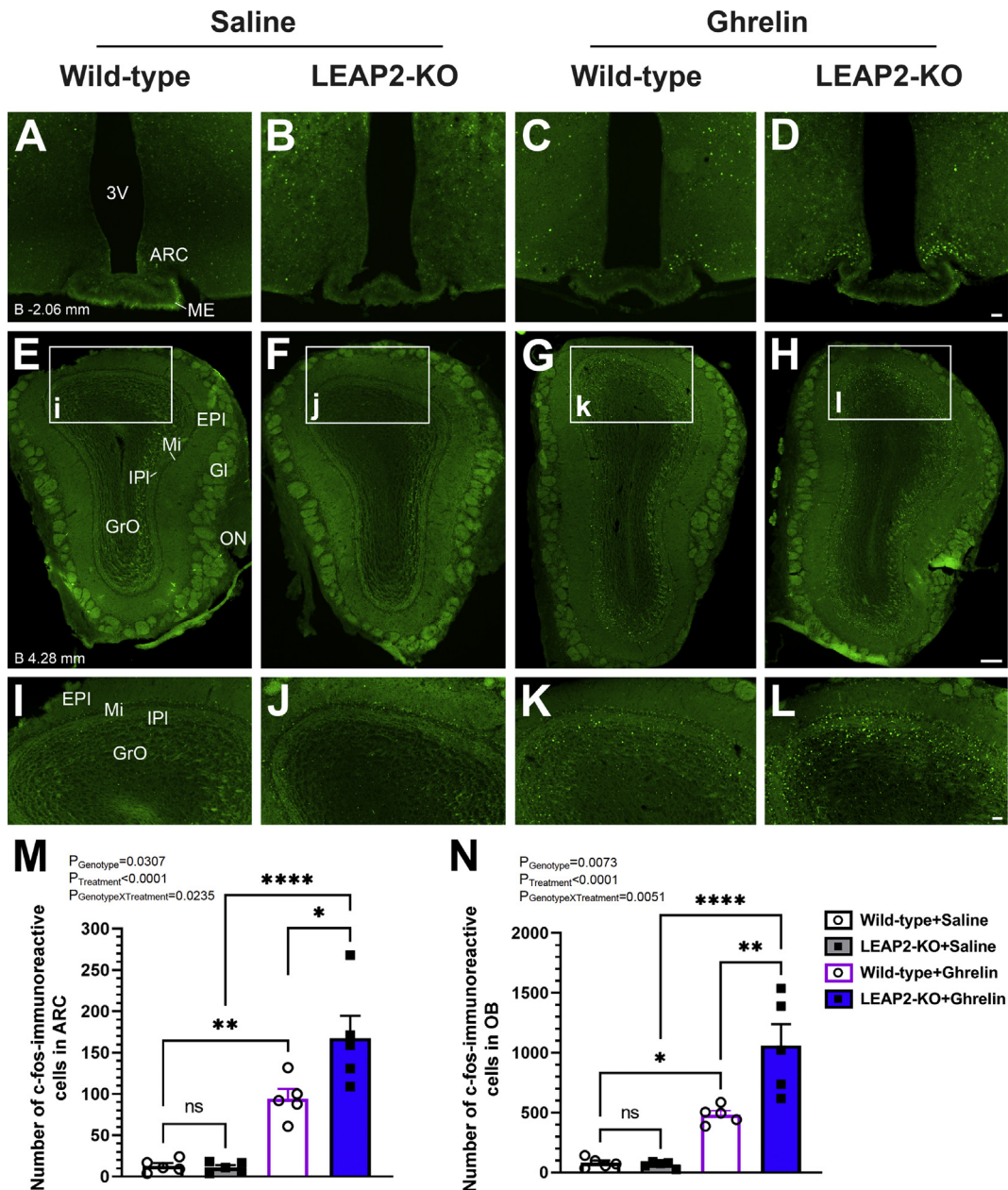
Figure 3: Effect of LEAP2 deletion on acyl-ghrelin-induced c-fos induction in the brain. Representative photomicrographs showing c-fos-immunoreactivity 2 h following administration of (**A-B**; **E-F**; **I-J**) saline or (**C-D**; **G-H**; **K-L**) acyl-ghrelin 0.5 mg/kg BW s.c. in the (**A-D**, **M**) arcuate hypothalamic nucleus (ARC; approximate distance from Bregma = −2.06 mm) and (**E-L**, **N**) olfactory bulb (OB; approximate distance from Bregma = 4.28) of (**A,C, E, G, I, K**) wild-type and (**B, D,F, H, J, L**) LEAP2-KO mice. (**I-L**) Magnified versions of the small rectangles labeled (**i-l**) in images (**E-H**). n = 5 mice for each genotype and each treatment. Numbers of c-fos-immunoreactive cells in (**M**) two levels of the ARC (bilaterally, approximately at Bregma = −1.82 and −2.06) and (**N**) one level of the OB (unilaterally, approximately at Bregma = 4.28) of wild-type and LEAP2-KO mice treated with saline or acyl-ghrelin. Data are presented as mean ± s.e.m. Data were analyzed by two-way ANOVA. *$P < 0.05$; **$P < 0.01$; and ****$P < 0.0001$. EPI, external plexiform layer; IPI, inner plexiform layer; GI, glomerular layer; GrO, granular cell layer; ME, median eminence; Mi, mitral cell layer; ON, olfactory nerve layer; 3V, ventricle. Scale bars = 50 μm in **A-D** and **I-L**; 200 μm in **E-H**.

over that observed in saline-treated mice, and no effect of LEAP2 deletion (Figure S2A—H). In addition, the scant numbers of c-fos-immunoreactive cells observed in the external lateral parabrachial nucleus, hippocampus, amygdala, piriform cortex, lateral septal nucleus, preoptic area, supraoptic area, dorsomedial hypothalamic nucleus, ventromedial hypothalamic nucleus, paraventricular thalamic nucleus, and supramamillary nucleus were unaffected by acyl-ghrelin treatment or genotype (Figure S2I—T and data not shown).

3.5. LEAP2 deletion does not impact rebound feeding following a 24-h fast

Following a 24-h fast, mice exhibit rebound hyperphagia, and at least some studies suggest that the rise in plasma acyl-ghrelin usually associated with the fast and/or GHSR constitutive activity contribute to that feeding phenotype [4,40,41]. Also of note, plasma LEAP2 levels drop during fasting then rise upon re-feeding [13], suggesting that the rise in plasma LEAP2 possibly might limit even greater acyl-ghrelin-

induced food intake upon re-feeding. Thus, we next sought to determine if LEAP2 deletion enhances rebound feeding following a 24-h fast. For these studies, we challenged 21–24 week-old male mice that were maintained on either standard chow diet or high-fat diet to a 24 h fast, after which their usual diet was re-introduced and food intake was determined over the next 24 h. No statistically significant, genotype-dependent differences in rebound food intake [of either standard chow (Figure 4A) or high-fat diet (Figure 4B)] were observed at 1 h, 2 h, 4 h, or 24 h following re-introduction of food after the 24-h fast.

3.6. LEAP2 deletion has no major effects on food intake, body weight, body composition, blood glucose, or body length in mice chronically fed standard chow diet

Whereas the above studies examined the effects of LEAP2 deletion on metabolic responses to rather acute manipulations, we next examined the effects of LEAP2 deletion on various metabolic parameters over a prolonged period of standard chow diet exposure. As indicated in Figure S1, both female and male wild-type and LEAP2-KO littermates were individually housed beginning at 4 weeks of age (1 week after weaning), when they were provided continuous *ad lib* exposure to standard chow diet (except as noted) for 16 weeks. Food intake and body weights were measured weekly. Body composition was determined monthly beginning at 4 weeks of age (females) or 8 weeks of age (males). Blood glucose level was measured monthly in the *ad lib*-fed state at 8 and 16 weeks of age and following a 24-h fast at 12 and 20 weeks of age. Plasma acyl-ghrelin and LEAP2 levels were determined at 16 weeks of age in the *ad lib*-fed state and at 20 weeks of age following a 24-h fast. Body lengths standard chow-fed females were determined at 22–25 weeks of age.

No differences in weekly food intake (Figure 5A and I), weekly body weights (Figure 5B and J), fat mass (Figure 5C and K), % fat mass, lean mass (Figure 5D and L), or % lean mass were observed between wild-type and LEAP2-KO mice in either female or male cohorts throughout the study period. Body lengths in standard chow-fed females also were genotype-independent (Figure 5E). *Ad lib*-fed, as well as 24-hr fasted blood glucose levels were genotype-independent in the female mice (Figure 5F). In male mice, *ad lib*-fed and 24-hr fasted blood glucose levels also were genotype-independent except for the 16-week-old *ad lib*-fed blood glucose level that was lower in LEAP2-KO mice as compared to wild-type littermates ($P < 0.05$), albeit

unlikely lower to a biologically-relevant degree (wild-type mice: 133 ± 4 mg/dL vs. LEAP2-KO mice: 120 ± 3 mg/dL; Figure 5M). Plasma acyl-ghrelin levels were not affected by LEAP2 deletion (Figure 5G and N).

Expectedly, plasma LEAP2 levels were markedly lower in LEAP2-KO mice compared to wild-type mice; this was the case for every animal tested (Figure 5H and O). The very low levels of plasma LEAP2 that were detected in LEAP2-KO mice (as opposed to zero levels of plasma LEAP2) at a minimum suggest a marked knockdown of LEAP2 expression instead of complete deletion of LEAP2 expression. However, genomic DNA sequencing demonstrating the absence of the LEAP2 coding sequence in these novel LEAP2-KO mice, plus their undetectable LEAP2 mRNA levels (Figure 1) argue for them being a true LEAP2-KO model with complete deletion of LEAP2 expression. We presume that the low levels of plasma LEAP2 detected in the LEAP2-KO mice instead occur as a result of cross-reactivity of the anti-LEAP2 antibody in the ELISA kit with a non-LEAP2 antigen that is present in low levels in the plasma. Of note, no regulation of the plasma LEAP2-like signal by diet or feeding status was observed in the LEAP2-KO mice, which further implies that the signal represents a non-LEAP2 antigen. In particular, values for male and female LEAP2-KO mice — whether exposed long-term to a high-fat diet or standard chow diet or whether in the *ad lib*-fed or 24 hr-fasted states — had a very narrow range between 2.5 ± 0.1 ng/mL to 3.1 ± 0.2 ng/mL, without statistically-significant P values (Figures 5H, O and 6H, O). This was unlike the expected [13] increased levels of plasma LEAP2 noted in wild-type mice as a consequence of long-term high-fat diet exposure vs. standard chow diet [for instance, *ad lib*-fed 16 week-old female wild-type mice on high-fat diet: 25.8 ± 2.4 ng/mL vs. standard chow diet: 12.9 ± 0.8 ng/mL, $P < 0.0001$ (Figure S3B); *ad lib*-fed 16 week-old male wild-type mice on high-fat diet: 24.4 ± 1.8 ng/mL vs. standard chow diet: 9.9 ± 0.5 ng/mL, $P < 0.0001$ (Figure S3G)]. In addition, this was unlike the expected [13] increased levels of plasma LEAP2 noted in wild-type mice as a consequence of the *ad lib*-fed state vs. a 24 h fast. Notably, we previously independently validated accurate detection of LEAP2 by the LEAP2 ELISA kit used here by demonstrating that the ELISA kit could reliably estimate the concentration of LEAP2 within assay buffer into which known amounts of LEAP2 are added [13]. Importantly, such validation does not preclude the potential detection of an additional, cross-reactive antigen in addition to LEAP2.
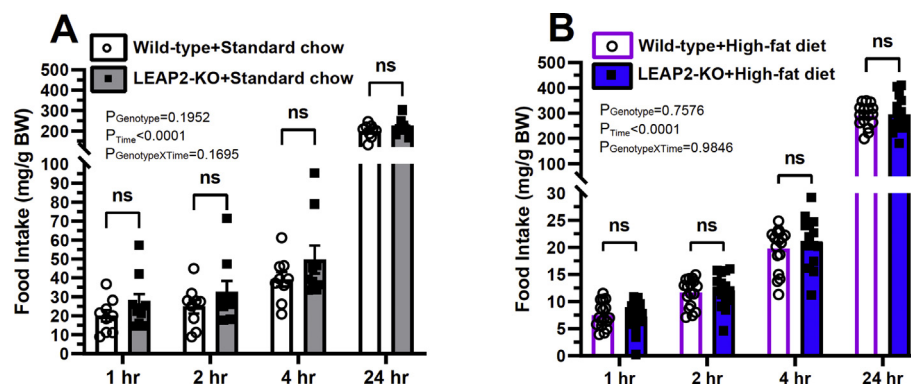

Figure 4: Effect of LEAP2 deletion on rebound feeding following a 24-hr fast. Food intake measured at 1 h, 2 h, 4 h, and 24 h following re-introduction of either **(A)** standard chow diet or **(B)** high-fat diet following a 24 h fast. n = 15–17. Data are presented as mean ± s.e.m. Data were analyzed by two-way repeated-measures ANOVA. ns represents no statistical significance.
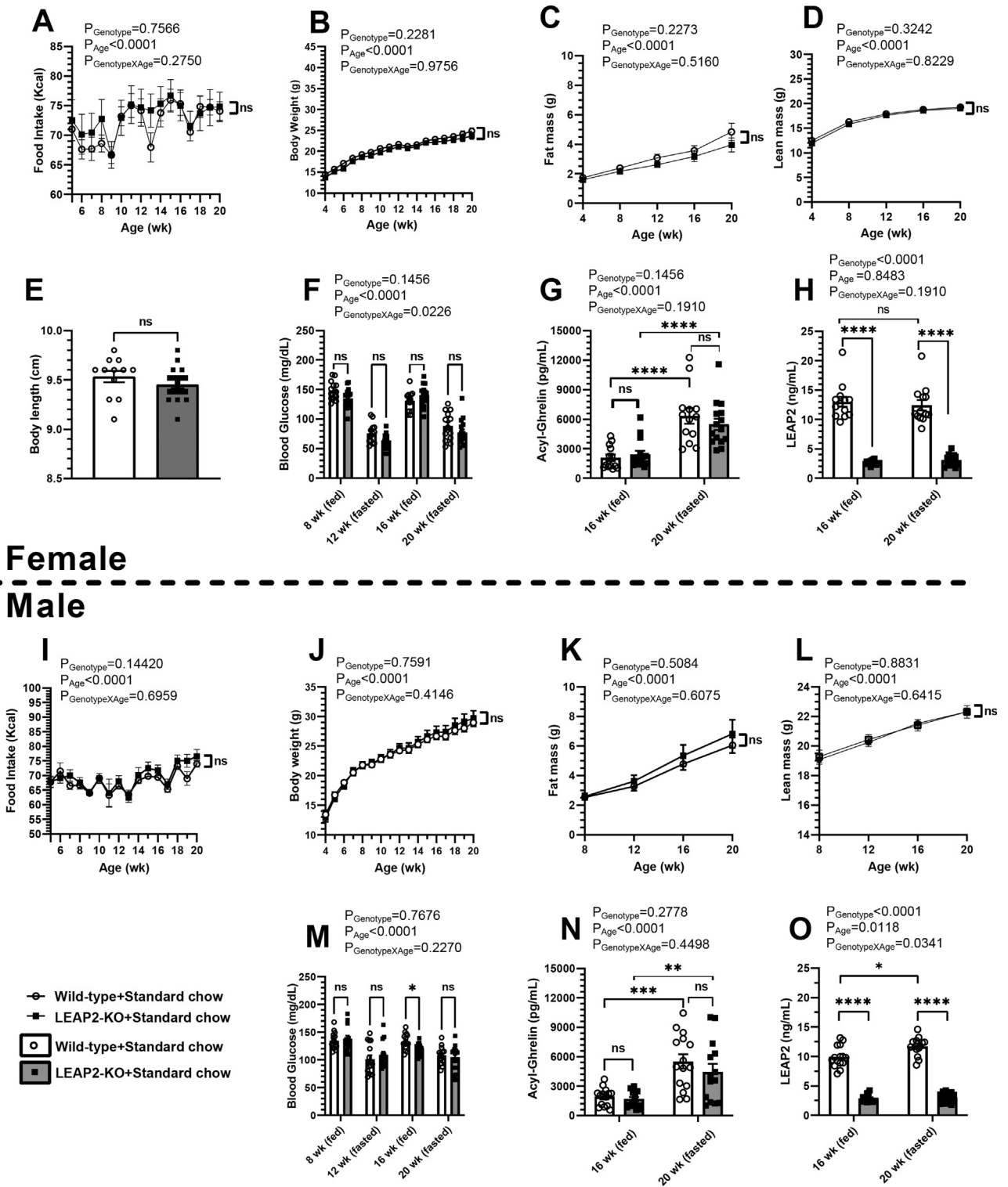
Figure 5: Metabolic impact of LEAP2 deletion on mice maintained long-term on a standard chow diet. (A, I) Weekly food intake, (B, J) weekly body weight, (C, K) monthly fat mass, (D, L) monthly lean mass, (E) body length measured at 22-25 weeks-of-age, (F, M) monthly blood glucose, (G, N) plasma acyl-ghrelin measured at 16 weeks of age (ad-lib fed) and 20 weeks of age (24 h fasted), and (H, O) plasma LEAP2 measured at 16 weeks of age (ad-lib fed) and 20 weeks-of-age (24 h fasted) in (A-H) females and (I—O) males. n = 13—15 females, n = 14—15 males. Data are presented as mean ± s.e.m. Data for (E) were analyzed by Student's t-test. All other data were analyzed by two-way repeated-measures ANOVA. ns represents no statistical significance between both genotypes. Statistically significant differences are indicated by asterisks: *$P < 0.05$; **$P < 0.01$; ***$P < 0.001$; and ****$P < 0.0001$.

3.7. LEAP2 deletion increases body weight, food intake, lean mass, and body length in female mice chronically fed a high-fat diet

A separate cohort of female and male LEAP2-KO mice and wild-type littermates instead was challenged long-term with a Western-type high-fat diet (42% kcal from fat). Except for the diet, all the above-mentioned protocols (in section 3.6) were followed in the current study. Weekly food consumption was found consistently higher in female LEAP2-KO mice than in female wild-type mice (on average, ~11% greater in LEAP2-KO mice; Figure 6A). Although female LEAP2-KO mice weighed similar to wild-type littermates at the commencement of the study, the LEAP2-KO mice gained more body weight than wild-type mice over the 16 weeks of feeding a high-fat diet (Figure 6B). After the study, female LEAP2-KO mice weighed 15% more than wild-type mice. Although after 16 weeks of high-fat diet feeding, fat mass in female LEAP2-KO mice was 18% higher than in female wild-type mice, over the course of the study, no statistically significant differences were observed (Figure 6C). After 16 weeks of the high-fat diet, lean mass in female LEAP2-KO mice was ~6% higher than in wild-type females, and over the course of the study, a statistically significant difference was observed (Figure 6D). Body lengths of high-fat diet-fed 23-24 week-old female LEAP2-KO mice were 1.7% more than those of wild-type littermates (Figure 6E). *Ad lib*-fed and 24 h fasted blood glucose levels obtained during the study period were unaffected by genotype in females (Figure 6F). In high-fat diet-fed females, plasma acyl-ghrelin levels were not affected by LEAP2 deletion (Figure 6G). Also, plasma LEAP2 antigenicity was detected only at very low levels in LEAP2-KO mice (Figure 6H; see section 3.6 for further discussion).

In males chronically fed the high-fat diet, LEAP2 deletion mostly did not affect the assessed metabolic parameters (Figure 6I—K and M—N). The one exception was the lean mass that was consistently slightly higher in the male LEAP2-KO mice than in the male wild-type littermates over the course of the study ($P = 0.09$) such that by the end of the study, it was ~4.4% higher in LEAP2-KO mice than in wild-type mice (Figure 6L). Similar to male and female LEAP2-KO mice fed standard chow and female LEAP2-KO mice fed high-fat diet, LEAP2 antigenicity detected in male LEAP2-KO mice fed on high-fat diet was very low (Figure 6O; section 3.6 for further discussion).

Although the absence of both *ad lib*-fed and 24-h fasted plasma samples from similarly-aged mice precludes us from assessing the effects of feeding status alone on plasma acyl-ghrelin and LEAP2 in the current study, we were able to determine the effects of diet on those hormone levels (Figure S3). Specifically, chronic high-fat diet reduced plasma acyl-ghrelin levels in both female and male wild-type mice and female and male LEAP2-KO mice in the fasted state (in 20 week-old mice); this effect of chronic high-fat diet on acyl-ghrelin was not apparent in the *ad lib*-fed state (in 16 week-old mice) (Figure S3A, D, F, I). As noted above, in wild-type mice, a chronic high-fat diet increased plasma LEAP2 levels in the *ad lib*-fed state in both females and males (aged 16 weeks old) (Figure S3B and G). In wild-type mice, a chronic high-fat diet also increased plasma LEAP2 levels in the fasted state in males but not females (aged 20 weeks) (Figure S3B and G). Altogether, these changes correspond to an effect of a chronic high-fat diet to raise the plasma LEAP2:acyl-ghrelin molar ratio in the *ad lib*-fed state in both female (by 173%) and male (by 402%) wild-type mice (aged 16 weeks), but not in the 24-h fasted state (in 20 week-old mice) (Figure S3C and H). It is unclear whether the effects of diet on hormone levels observed are due to direct effects of the macronutrients contained within the diets, the effects of the diet on body weight, the effects of the diet on body composition, or a combination of those effects. There was no effect of diet on the low LEAP2 antigenicity detected in LEAP2-KO mice (Figure S3E and J).

3.8. Female mice lacking LEAP2 exhibit decreased energy expenditure and locomotor activity

Another cohort of 8-week-old female mice that had been on a high-fat diet for 4 weeks was placed in a metabolic chamber system in order to assess any genotype-dependent differences in measures of energy expenditure, locomotor activity, and meal patterning. We compared the performance of the two genotypes throughout the first 5 h of the light cycle, and the first 5 h of the dark cycle, as well during the total 24 h period, the total 12-hr dark cycle, and the total 12-hr light cycle. LEAP2-KO mice demonstrated statistically significant reductions in O_2 consumption (on average, a 13% reduction in LEAP2-KO mice vs. wild-type mice; Figure 7A and D) and locomotor activity (on average, a 49% reduction in LEAP2-KO mice vs. wild-type mice; Figure 7B and E) during the first 5 h of the dark cycle. Heat production also was reduced (by 9.5%) in LEAP2-KO mice vs. wild-type mice during the first 5 h of the dark cycle (Figure 7C and F). No genotype-dependent differences were observed in CO_2 production (Figure 7G and I), respiratory exchange ratio (RER; Figure 7H and J), average meal size (Figure 7K), biggest meal (Figure 7L), or total food consumed (Figure 7M) during the first 5 h of the dark cycle. However, LEAP2-KO mice exhibited a slight reduction in the number of meals consumed during the first 5 h of the dark cycle (on average, from 10 to 8; Figure 7N). No differences in O_2 consumption, locomotor activity, heat production, CO_2 production, RER, average meal size, biggest meal, total food consumed, or the number of meals consumed were otherwise detected during the first 5 h of light (Figure 7), the total light period, the total dark period, or the total 24 h period.

3.9. LEAP2 deletion increases hepatic lipid accumulation in high-fat diet-fed mice

Finally, we determined the effect of LEAP2 deletion on liver histology. Liver tissue sections from 22 to 24 week-old female mice taken from the long-term standard chow and high-fat diet feeding studies described above (sections 3.6 and 3.7) were stained with hematoxylin & eosin or oil red O. There was no effect of genotype on hepatic fat accumulation in standard chow-fed mice (Figure 8A—D). A high-fat diet increased hepatic fat accumulation in both genotypes, although this was more pronounced in LEAP2-KO mice (Figure 8B and C). Specifically, in high-fat diet-fed mice, a 42% increase in the oil red O-positive area in LEAP2-KO livers over that in wild-type livers was observed (Figure 8B). Also, although there was not an overall genotype-dependent difference in lipid droplet number in the high-fat diet-fed mice (Figure 8C), there were statistically significant increases in the numbers of larger lipid droplets in LEAP2-KO mice than in wild-type littermates (271% and 1,464% increases in numbers of lipid droplets sized 15,000—30,000 μm^2 and >30,000 μm^2, respectively; Figure 8E).

4. DISCUSSION

To our knowledge, this study represents the first report of a LEAP2-KO mouse model. LEAP2-KO mice exhibited increased sensitivity to the actions of administered acyl-ghrelin to stimulate GH secretion, induce food intake, and activate cells in the ARC and OB. This was particularly evident in diet-induced obesity, in which not even an exceedingly high dose of acyl-ghrelin [33] could acutely stimulate food intake in wild-type mice, relative to the 10× lower dose of acyl-ghrelin that stimulated food intake in LEAP2-KO littermates. No observable or prominent effects of LEAP2 deletion on food intake, body weight, body composition, or blood glucose were recorded in standard chow-fed female and male mice up to 26 weeks of age or high-fat diet-fed male mice up
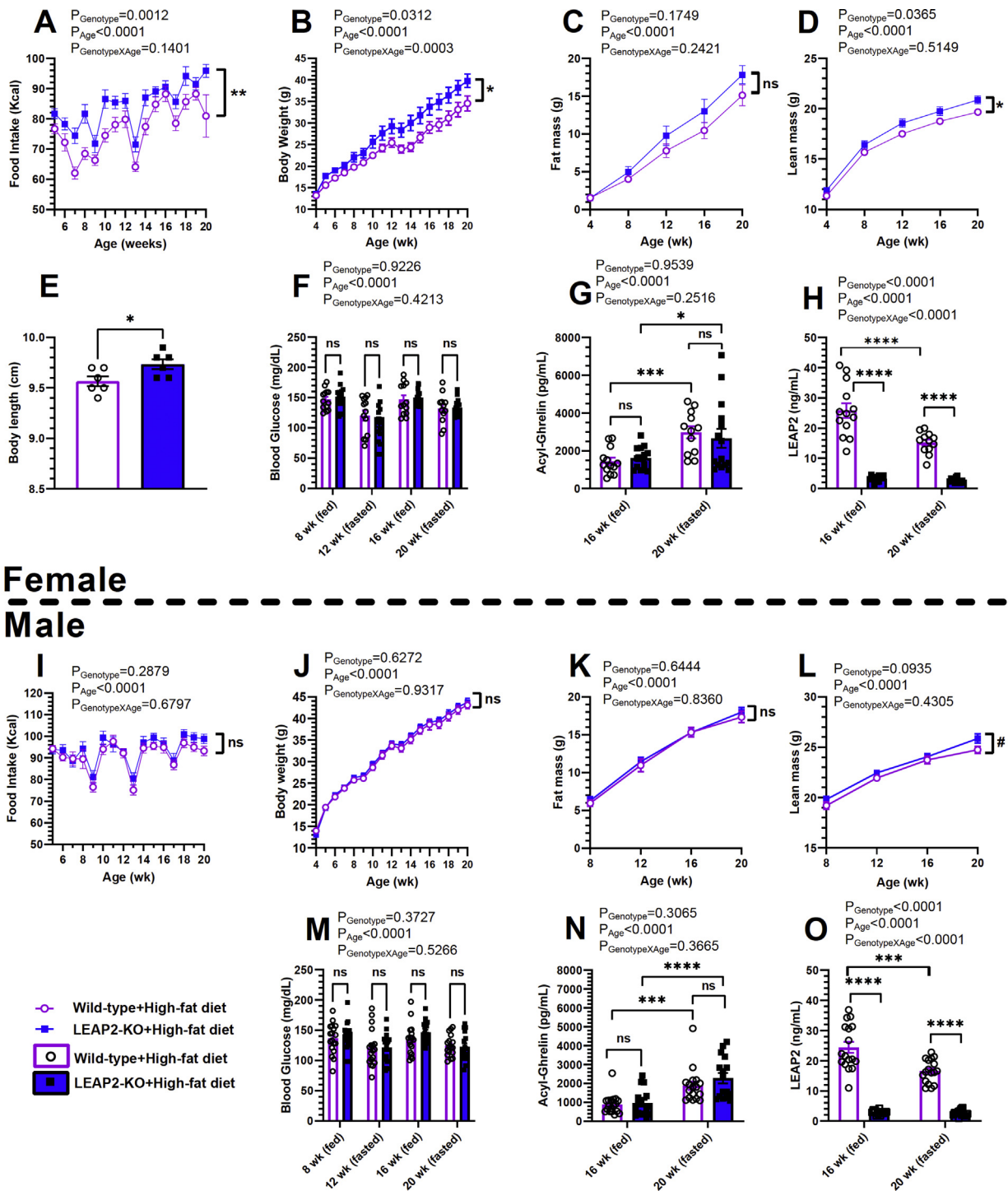
Figure 6: Metabolic impact of LEAP2 deletion on mice challenged long-term with high-fat diet (HFD). (A, I) Weekly food intake, (B, J) weekly body weight, (C, K) monthly fat mass, (D, L) monthly lean mass, (E) body length measured at 22−25 weeks of age, (F, M) monthly blood glucose, (G, N) plasma acyl-ghrelin measured at 16 weeks of age (*ad-lib* fed) and 20 weeks of age (24 h fasted), and (H, O) plasma LEAP2 measured at 16 weeks-of-age (*ad-lib* fed) and 20 weeks-of-age (24 h fasted) in (A-H) females and (I−O) males. n = 13−15 females; n = 17−18 males. Data are presented as mean ± s.e.m. Data for (E) were analyzed by Student's t-test. All other data were analyzed by two-way repeated-measures ANOVA. Statistically significant differences are indicated by asterisks: *$P < 0.05$; **$P < 0.01$; ***$P < 0.001$; and ****$P < 0.0001$. ns represents no statistical significance. #$P \geq 0.05$ but < 0.1.

to 24 weeks of age. Also, no observable effects of LEAP2 deletion on rebound food intake following a 24-hr fast were recorded in ∼6 month-old male mice. Yet, LEAP2 deletion did impact several metabolic parameters in high-fat diet-fed female mice. Specifically, over the course of a 16-week chronic high-fat diet feeding study, female LEAP2-KO mice consistently exhibited increased weekly food intake (on average, 7.8 kcal more per week) and gained on average 3.6 g more bodyweight, as well as more lean mass and more hepatic fat than wild-
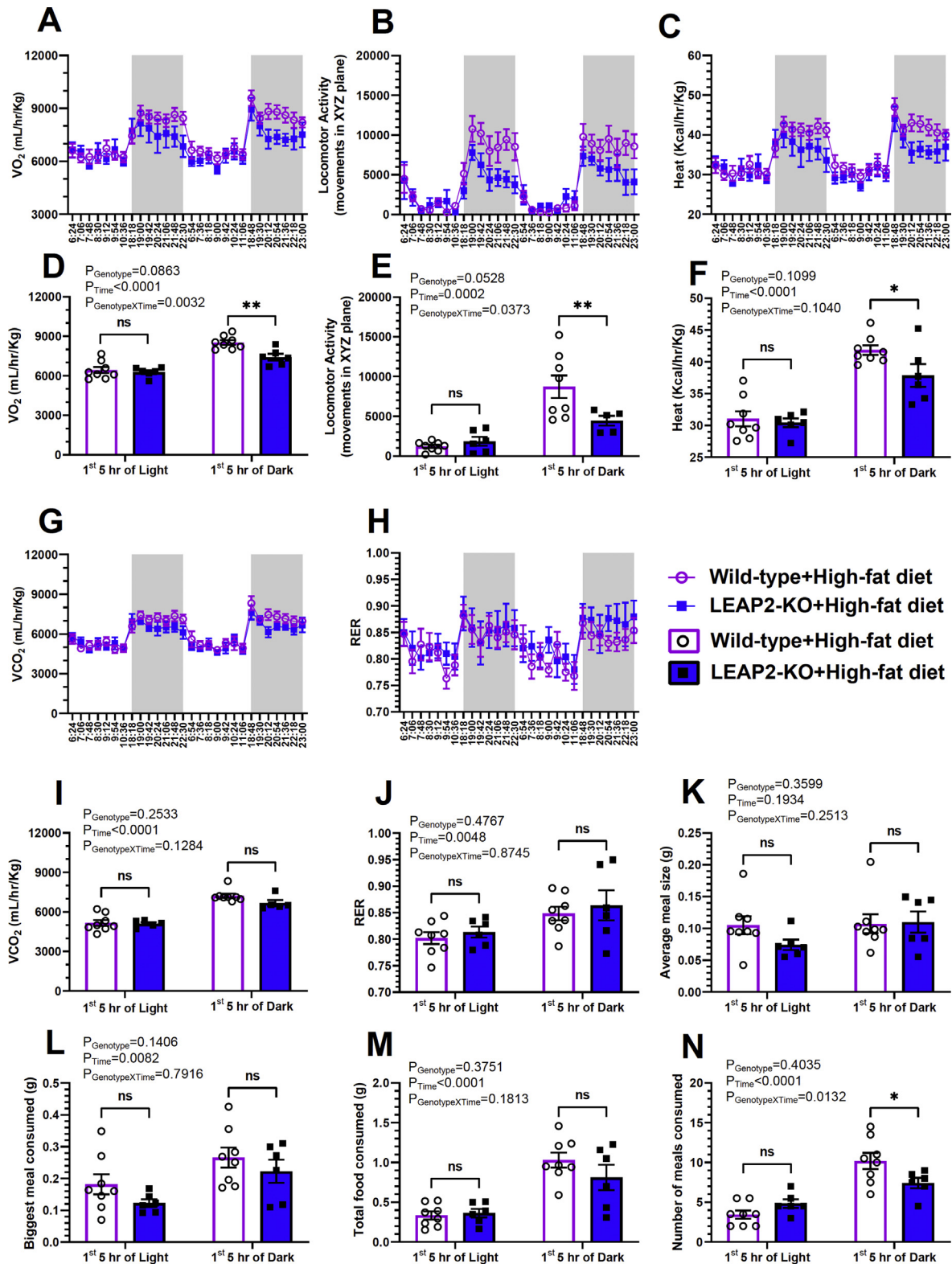
Figure 7: Metabolic chamber data in high-fat diet-fed female mice. Oxygen consumption (**A**, **D**), Locomotor activity in the x, y, and z planes (**B**, **E**), heat production (**C**, **F**), CO_2 production (**G**, **I**), RER (**H**, **J**). Average meal size (**K**), the maximum meal consumed (**L**), total food consumed (**M**), and the number of meals consumed. n = 6−8. Data were obtained in 8 week-old mice that had been exposed to a high-fat diet since 4 weeks of age. The data in **A-C** and **G-H** represent the mean ± s.e.m. over the final two full light cycles and dark cycles (highlighted by gray rectangles). The data in **D-F** and **I—N** represent the mean ± s.e.m. for the 1st 5 h of the light cycles and the 1 st 5 h of the dark cycles. Data were analyzed by two-way repeated-measures ANOVA. Statistically significant differences between LEAP2-KO and wild-type mice are indicated by asterisks; *$P < 0.05$; **$P < 0.01$. ns represents no statistical significance.
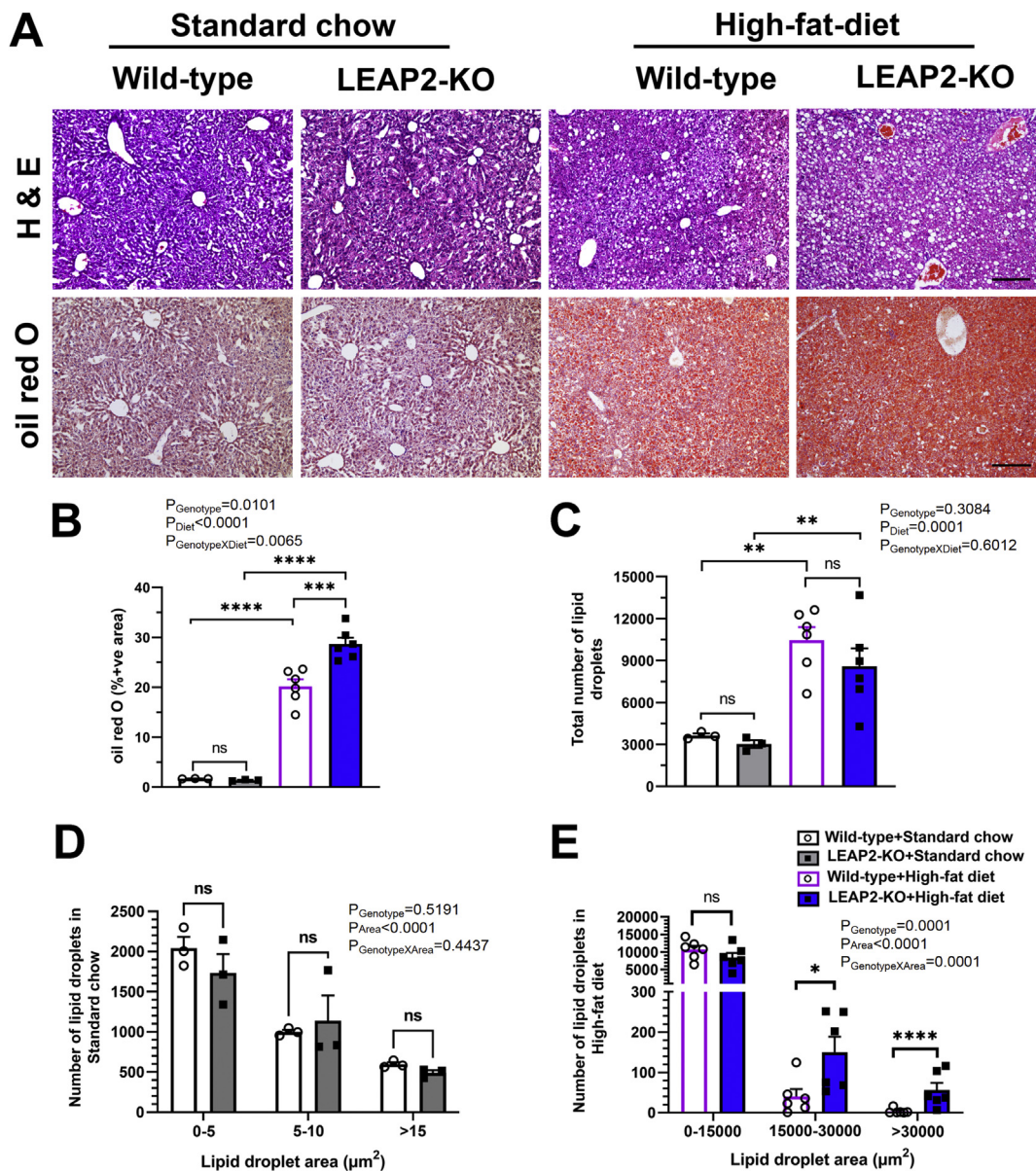
Figure 8: Effect of LEAP2 deletion on liver histology and hepatic fat accumulation. (A) Representative photomicrographs of livers stained with **(Upper panels)** Hematoxylin & eosin (H & E) and **(Lower panels)** oil red O from Wild-type and LEAP2-KO mice fed long-term with standard chow diet or high-fat diet. (B) Quantification of the percentage of the tissue area that contains oil red O staining. (C) The total number of lipid droplets in standard chow-fed and high-fat diet-fed mice. (D) A number of lipid droplets of different size range in standard chow-fed mice. (E) The number of lipid droplets of different size ranges in high-fat diet-fed mice. n = 3 per genotype of standard chow-fed mice; n = 6 per genotype of high-fat diet-fed mice. Data are presented as mean ± s.e.m. Data were analyzed by two-way ANOVA. Statistically significant differences are indicated by asterisks; *$P < 0.05$; **$P < 0.01$, ***$P < 0.001$, ****$P < 0.0001$. ns represents no statistical significance.

type littermates. When placed in metabolic cages after only 4 weeks of high-fat diet exposure [which was several weeks prior to the more obvious divergence in body weight and body composition observed later (for instance, at 12 - 13 weeks-of-age)], the female LEAP2-KO mice had reduced O_2 consumption, heat production, and locomotor activity in the first part of the dark cycle. This suggests decreased energy expenditure during the period when mice typically are most active. Additionally, LEAP2 deletion significantly increased body length (on average, by 1.6 mm) in high-fat diet-fed female mice as compared to wild-type littermates when measured at 23—24 weeks of age.

A prominent finding of the current study was the increased sensitivity to administered acyl-ghrelin observed in the LEAP2-KO mice.

Specifically, the observed orexigenic responses in LEAP2-KO mice to acyl-ghrelin doses that were ineffective in wild-type mice, particularly in mice chronically fed high-fat diet, supports the hypothesis that LEAP2 is a key determinant of ghrelin resistance. Also supporting this hypothesis, LEAP2-KO mice exhibited increased ARC and OB c-fos-immunoreactivity and increased plasma GH following acyl-ghrelin administration. These novel findings support and bolster the findings of Ge et al. in which administration of anti-LEAP2 neutralizing antibodies raised plasma GH [1]. These new results also fit the expected outcomes for deleting LEAP2 given its reported actions as a potent GHSR antagonist in multiple *in vitro*, *ex vivo*, and *in vivo* studies [1,9—13]. Certainly, the findings of decreased energy expenditure and

greater weekly food intake, body weight, and lean mass in high-fat diet-fed female LEAP2-KO mice also support the assertion that LEAP2 deletion alleviates the ghrelin resistance that is most notable in the diet-induced obese state. Yet, it remains unclear why more robust effects on food intake, body weight, and body composition were not detected in LEAP2-KO mice following long-term exposure of males and females to a standard chow diet or of males to a high-fat diet.

One intriguing clue to the cause of the discrepancy between the metabolic outcomes of LEAP2 deletion in high-fat diet-fed females vs. high-fat diet-fed males may be the different mean plasma acyl-ghrelin levels observed in those two groups. For example, 16 week-old, *ad lib*-fed female LEAP2-KO mice had on average 68% more plasma acyl-ghrelin than 16 week-old, *ad lib*-fed male LEAP2-KO mice ($P < 0.01$; Figure 6G and N). If GHSR signaling acts substantively to decrease energy expenditure, increase food intake, and increase body weight, and if GHSR signaling is enhanced by lower plasma LEAP2 plus higher plasma acyl-ghrelin, then the higher plasma acyl-ghrelin in high-fat diet-fed female LEAP2-KO mice could help explain the magnified metabolic effects of LEAP2 deletion in the females vs. males. Notably, previous studies also have identified sexually dimorphic effects of GHSR deletion on body weight and body composition, along with estrogen-dependent changes in plasma ghrelin levels, acyl-ghrelin orexigenic efficacy, and arcuate hypothalamic *Ghsr* expression [36,42,43]. Future studies in which acyl-ghrelin is administered chronically to high-fat diet-fed LEAP2-KO males, in order to generate plasma acyl-ghrelin levels similar to those observed in high-fat diet-fed LEAP2-KO females, might help test this hypothesis.

Another finding of interest in the current study was the increased hepatic fat accumulation in high-fat diet-fed female LEAP2-KO mice vs. wild-type mice. Specifically, 29% of the imaged liver area was oil red O-positive in LEAP2-KO mice vs. 20% in wild-type littermates. Plus, livers from high-fat diet-fed female LEAP2-KO mice contained marked increases in the numbers of lipid droplets sized >15,000 μm^2. Although this result contradicts the observations of reduced hepatic oil red O staining and hepatic triglyceride content reported by Ma et al., in which lentivirus delivery of an shRNA-*Leap2* construct was used to knockdown *Leap2* expression in high-fat diet-fed female mice [14], differences in the duration of exposure to reduced LEAP2, the degree of LEAP2 knockdown (plasma LEAP2 was reduced by only about 60% in [14]), and possibly also the development of pathways that might compensate for reduced LEAP2 might help explain these discrepancies in hepatic fat accumulation. Nonetheless, other studies demonstrating increased hepatic steatosis upon GHSR agonism vs. reduced hepatic fat content upon GHSR antagonism or GHSR inverse agonism correspond with the findings here of increased hepatic fat in the high-fat diet-fed female LEAP2-KO mice. For instance, Davies et al., Li et al., and Dallak showed that 1—2 weeks of acyl-ghrelin administration induced hepatic steatosis in lean rats, lean mice, and/or diet-induced obese mice [44—46]. Zhang et al. demonstrated that knockdown or inhibition of ghrelin-*O*-acyltransferase, the enzyme that acylates ghrelin and thus permits it to effectively interact with GHSR, decreased hepatic triglyceride content and oil red O staining in high-fat diet-fed mice [47]. Abegg et al. demonstrated substantial decreases in hepatic fat content in diet-induced mice upon 10-d of administered synthetic GHSR inverse agonist [48]. In Li et al., administration of a synthetic GHSR antagonist for 1 week markedly reduced hepatic triglyceride content, oil red O staining, and expression of several genes related to hepatic lipogenesis in diet-induced obese mice [46]. In neither of the last two studies were the effects of the GHSR antagonist or GHSR inverse agonist related to effects on food intake [46,48]. Li et al. also demonstrated reduced hepatic oil red O staining and triglyceride content in high-fat diet-fed GHSR-knockout mice as compared to wild-type littermates [46]. Similarly, Guillory et al. demonstrated that standard non-soy chow-fed ghrelin-KO mice aged 20 months had significantly less hepatic steatosis than age-matched wild-type mice [49]. Notably, this difference was not apparent in younger (3 month-old) mice [49] suggesting that certain effects of acyl-ghrelin or LEAP2 might only become obvious or might be most apparent upon aging. Future studies comparing older standard chow-fed LEAP2-KO and wild-type littermates or older high-fat diet-fed male LEAP2-KO and wild-type littermates might help test such a hypothesis. Altogether, these findings, alongside the previously reported robust association of intrahepatocellular lipid content with plasma LEAP2 in human subjects [13,14], suggest that LEAP2 may act as part of a physiologic feedback mechanism that helps mitigate steatosis in obesogenic conditions.

Finally, it is noteworthy that s.c. acyl-ghrelin administration to LEAP2-KO mice induced greater c-fos expression not only in the ARC but also in the OB. First, regarding our objective analyses of the c-fos data, all statistical tests for ARC and OB (main effects of genotype and treatment and their interaction in two-way ANOVA models) were statistically significant. The statistical significance at alpha = 0.05, with a sample size of 5 per group (total = 20), clearly demonstrates high power for these inferences. However, to get an initial estimate of post hoc power, we calculated partial eta squared for each test and associated power based on these observed effect sizes. Partial eta squared estimates ranged from 0.26 to 0.80 and corresponding power ranged from 0.70 to 1.00. However, it should be noted that post hoc power analyses based on observed effects sizes with small sample size is limited in scope and interpretation due to the high variance in the estimated effect sizes and subsequent power calculations. Second, to our knowledge, acyl-ghrelin-induced c-fos induction in the OB has not yet been reported. One study however did report that nasal application of an acyl-ghrelin solution nearly doubled the percentage of c-fos-positive juxtaglomerular OB cells in mice induced by the odorant 2,3-hexanedione [50], and another study demonstrated that caloric restriction induces c-fos in new adult-born OB cells in a ghrelin-dependent manner [51]. While the role of ARC as a direct target of acyl-ghrelin action has long been acknowledged and explored in several studies [30,32,39,52—54], the OB as a target of acyl-ghrelin action has received less attention. Even so, several relevant findings regarding GHSR expression and acyl-ghrelin action in the OB have been reported. For instance, Tong et al. described moderate to high expression of a GHSR promoter-driven beta-galactosidase reporter in the glomerular, mitral cell, and granular cell layers of the main OB and in the accessory OB of mice as well as biotinylated ghrelin binding to scattered cells within the OB of sectioned rat brains [55]. GHSR expression in the OB has been reported in GHSR-eGFP transgenic mice [29,51] and guinea pigs [56]. Additionally, two studies demonstrated that the OB represents the brain area with the highest or one of the top two highest distributions of radiolabeled-acyl-ghrelin acutely following its i.v. administration [57,58]. These findings suggest that acyl-ghrelin might modulate olfactory behaviors. Administered acyl-ghrelin was shown to stimulate exploratory sniffing and increase olfactory sensitivity using rat and human models [55]. Future studies using radiolabeled or fluorescein-labeled LEAP2 analogs similar to those described for acyl-ghrelin [57—60] could help confirm whether LEAP2 penetrates the OB, as suggested by the current findings. Also, OB-selective GHSR knockout studies may help clarify the biological significance of acyl-ghrelin and LEAP2 action in the OB.

5. CONCLUSIONS

These data reveal that LEAP2 deletion sensitizes mice to the actions of peripherally administered acyl-ghrelin to acutely increase food intake, stimulate GH secretion, and induce c-fos in the ARC and OB. Also, our findings show that LEAP2 deletion decreases energy expenditure and increases weekly food intake, body weight, lean mass, hepatic fat accumulation, and body length in high-fat diet-fed female mice, but has no biologically significant effects on those parameters in high-fat diet-fed male mice or standard chow-fed female and male mice. Whether these effects in high-fat diet-fed female mice are a function of a loss of LEAP2's usual effects to block acyl-ghrelin action and/or to reduce GHSR constitutive activity remains to be determined. Also, whether the physiologic effects of deleting the *Leap2* gene observed here are solely due to loss of the 40 amino acid-long mature LEAP2 hormone or additionally to loss of other predicted or proven smaller peptide derivatives of the LEAP2 preprohormone precursor [18] awaits investigation.

CONTRIBUTION STATEMENT

KS performed the acyl-ghrelin administrations, fast/re-refeeding, blood collection, ELISA assays, tissue harvests, and statistical analyses and helped write the manuscript. NPM performed the long-term feeding studies. OS performed tissue harvests, histology, and helped write the manuscript. BKM helped design the study, perform the initial valida-tions of the LEAP2-KO line, and write the manuscript. SOL designed the strategy to generate the LEAP2-KO line, validated the line, per-formed PCR, and helped write the manuscript. SV, DG, and ST assisted with performing the studies. SBO assisted with performing the studies, statistical analyses, and editing the manuscript. CPR worked with NPM to organize the breeding schedule and all aspects of animal husbandry required for the study. KN performed the statistical analyses and power analyses for the c-fos induction studies and helped write the related parts of the manuscript. CL monitored the generation of the LEAP2-KO line. JMZ designed the study and oversaw all other aspects of the study, helped write the manuscript, and secured funding. All authors approved the final version.

CONFLICT OF INTEREST

BKM is currently employed by Novo Nordisk Research Center Indianapolis, Inc., although his major contributions to the study occurred while on faculty at UT Southwestern Medical Center. The other authors have no conflicts of interest.

APPENDIX A. SUPPLEMENTARY DATA

Supplementary data to this article can be found online at https://doi.org/10.1016/j.molmet.2021.101327.

REFERENCES

[1] Ge, X., Yang, H., Bednarek, M.A., Galon-Tilleman, H., Chen, P., Chen, M., et al., 2018. LEAP2 is an endogenous antagonist of the ghrelin receptor. Cell Metabolism 27(2):461–469 e466.

[2] Krause, A., Sillard, R., Kleemeier, B., Kluver, E., Maronde, E., Conejo-Garcia, J.R., et al., 2003. Isolation and biochemical characterization of LEAP-2, a novel blood peptide expressed in the liver. Protein Science 12(1):143–152.

[3] Howard, A., Townes, C., Milona, P., Nile, C.J., Michailidis, G., Hall, J., 2010. Expression and functional analyses of liver expressed antimicrobial peptide-2 (LEAP-2) variant forms in human tissues. Cellular Immunology 261(2):128–133.

[4] Mani, B.K., Osborne-Lawrence, S., Vijayaraghavan, P., Hepler, C., Zigman, J.M., 2016. beta1-Adrenergic receptor deficiency in ghrelin-expressing cells causes hypoglycemia in susceptible individuals. Journal of Clinical Investigation 126(9):3467–3478.

[5] Li, R.L., Sherbet, D.P., Elsbernd, B.L., Goldstein, J.L., Brown, M.S., Zhao, T.J., 2012. Profound hypoglycemia in starved, ghrelin-deficient mice is caused by decreased gluconeogenesis and reversed by lactate or fatty acids. Journal of Biological Chemistry 287(22):17942–17950.

[6] Zhang, Y., Fang, F., Goldstein, J.L., Brown, M.S., Zhao, T.J., 2015. Reduced autophagy in livers of fasted, fat-depleted, ghrelin-deficient mice: reversal by growth hormone. Proceedings of the National Academy of Sciences of the United States of America 112(4):1226–1231.

[7] Zhao, T.J., Liang, G., Li, R.L., Xie, X., Sleeman, M.W., Murphy, A.J., et al., 2010. Ghrelin O-acyltransferase (GOAT) is essential for growth hormone-mediated survival of calorie-restricted mice. Proceedings of the National Academy of Sciences of the United States of America 107(16):7467–7472.

[8] McFarlane, M.R., Brown, M.S., Goldstein, J.L., Zhao, T.J., 2014. Induced ablation of ghrelin cells in adult mice does not decrease food intake, body weight, or response to high-fat diet. Cell Metabolism 20(1):54–60.

[9] Islam, M.N., Mita, Y., Maruyama, K., Tanida, R., Zhang, W., Sakoda, H., et al., 2020. Liver-expressed antimicrobial peptide 2 antagonizes the effect of ghrelin in rodents. Journal of Endocrinology 244(1):13–23.

[10] M'Kadmi, C., Cabral, A., Barrile, F., Giribaldi, J., Cantel, S., Damian, M., et al., 2019. N-terminal liver-expressed antimicrobial peptide 2 (LEAP2) region ex-hibits inverse agonist activity toward the ghrelin receptor. Journal of Medicinal Chemistry 62(2):965–973.

[11] Barrile, F., M'Kadmi, C., De Francesco, P.N., Cabral, A., Garcia Romero, G., Mustafa, E.R., et al., 2019. Development of a novel fluorescent ligand of growth hormone secretagogue receptor based on the N-Terminal Leap2 re-gion. Molecular and Cellular Endocrinology 498:110573.

[12] Cornejo, M.P., Castrogiovanni, D., Schioth, H.B., Reynaldo, M., Marie, J., Fehrentz, J.A., et al., 2019. Growth hormone secretagogue receptor sig-nalling affects high-fat intake independently of plasma levels of ghrelin and LEAP2, in a 4-day binge eating model. Journal of Neuroendocrinology 31(10):e12785.

[13] Mani, B.K., Puzziferri, N., He, Z., Rodriguez, J.A., Osborne-Lawrence, S., Metzger, N.P., et al., 2019. LEAP2 changes with body mass and food intake in humans and mice. Journal of Clinical Investigation 129(9):3909–3923.

[14] Ma, X., Xue, X., Zhang, J., Liang, S., Xu, C., Wang, Y., et al., 2020. Liver expressed antimicrobial peptide 2 is associated with steatosis in mice and humans. Experimental and Clinical Endocrinology & Diabetes 129(8):601–610.

[15] Barja-Fernandez, S., Lugilde, J., Castelao, C., Vazquez-Cobela, R., Seoane, L.M., Dieguez, C., et al., 2021. Circulating LEAP-2 is associated with puberty in girls. International Journal of Obesity 45(3):502–514.

[16] Aslanipour, B., Alan, M., Demir, I., 2020. Decreased levels of liver-expressed antimicrobial peptide-2 and ghrelin are related to insulin resistance in women with polycystic ovary syndrome. Gynecological Endocrinology 36(3): 222—225.

[17] Fittipaldi, A.S., Hernandez, J., Castrogiovanni, D., Lufrano, D., De Francesco, P.N., Garrido, V., et al., 2020. Plasma levels of ghrelin, des-acyl ghrelin and LEAP2 in children with obesity: correlation with age and insulin resistance. European Journal of Endocrinology 182(2):165—175.

[18] Hagemann, C.A., Zhang, C., Hansen, H.H., Jorsal, T., Rigbolt, K.T.G., Madsen, M.R., et al., 2021. Identification and metabolic profiling of a novel human gut-derived LEAP2 fragment. Journal of Clinical Endocrinology & Metabolism 106(2):e966—e981.

[19] Francisco, V., Tovar, S., Conde, J., Pino, J., Mera, A., Lago, F., et al., 2020. Levels of the novel endogenous antagonist of ghrelin receptor, liver-enriched antimicrobial peptide-2, in patients with rheumatoid arthritis. Nutrients 12(4):1006.

[20] Gupta, D., Ogden, S.B., Shankar, K., Varshney, S., Zigman, J.M., 2021. A LEAP 2 conclusions? Targeting the ghrelin system to treat obesity and diabetes. Molecular Metabolism 46:101128.

[21] Cornejo, M.P., Mustafa, E.R., Cassano, D., Baneres, J.L., Raingo, J., Perello, M., 2021. The ups and downs of growth hormone secretagogue receptor signaling. FEBS Journal. https://doi.org/10.1111/febs.15718.

[22] Andrews, Z.B., 2019. The next big LEAP2 understanding ghrelin function. Journal of Clinical Investigation 129(9):3542—3544.

[23] Zigman, J.M., Bouret, S.G., Andrews, Z.B., 2016. Obesity impairs the action of the neuroendocrine ghrelin system. Trends in Endocrinology and Metabolism 27(1):54—63.

[24] Perreault, M., Istrate, N., Wang, L., Nichols, A.J., Tozzo, E., Stricker-Krongrad, A., 2004. Resistance to the orexigenic effect of ghrelin in dietary-induced obesity in mice: reversal upon weight loss. International Journal of Obesity and Related Metabolic Disorders 28:879—885.

[25] Martin, N.M., Small, C.J., Sajedi, A., Patterson, M., Ghatei, M.A., Bloom, S.R., 2004. Pre-obese and obese agouti mice are sensitive to the anorectic effects of peptide YY(3-36) but resistant to ghrelin. International Journal of Obesity and Related Metabolic Disorders 28(7):886—893.

[26] Gardiner, J.V., Campbell, D., Patterson, M., Kent, A., Ghatei, M.A., Bloom, S.R., et al., 2010. The hyperphagic effect of ghrelin is inhibited in mice by a diet high in fat. Gastroenterology 138(7):2468—2476, 2476 e2461.

[27] Naznin, F., Toshinai, K., Waise, T.M., NamKoong, C., Md Moin, A.S., Sakoda, H., et al., 2015. Diet-induced obesity causes peripheral and central ghrelin resistance by promoting inflammation. Journal of Endocrinology 226(1):81—92.

[28] Tamboli, R.A., Antoun, J., Sidani, R.M., Clements, A., Harmata, E.E., Marks-Shulman, P., et al., 2017. Metabolic responses to exogenous ghrelin in obesity and early after Roux-en-Y gastric bypass in humans. Diabetes, Obesity and Metabolism 19(9):1267—1275.

[29] Mani, B.K., Walker, A.K., Lopez Soto, E.J., Raingo, J., Lee, C.E., Perello, M., et al., 2014. Neuroanatomical characterization of a growth hormone secretagogue receptor-green fluorescent protein reporter mouse. Journal of Comparative Neurology 522(16):3644—3666.

[30] Wang, Q., Liu, C., Uchida, A., Chuang, J.C., Walker, A., Liu, T., et al., 2014. Arcuate AgRP neurons mediate orexigenic and glucoregulatory actions of ghrelin. Molecular Metabolism 3(1):64—72.

[31] Tan, K., Knight, Z.A., Friedman, J.M., 2014. Ablation of AgRP neurons impairs adaption to restricted feeding. Molecular Metabolism 3(7):694—704.

[32] Briggs, D.I., Enriori, P.J., Lemus, M.B., Cowley, M.A., Andrews, Z.B., 2010. Diet-induced obesity causes ghrelin resistance in arcuate NPY/AgRP neurons. Endocrinology 151(10):4745—4755.

[33] Chuang, J.C., Sakata, I., Kohno, D., Perello, M., Osborne-Lawrence, S., Repa, J.J., et al., 2011. Ghrelin directly stimulates glucagon secretion from pancreatic alpha-cells. Molecular Endocrinology 25(9):1600—1611.

[34] Torz, L.J., Osborne-Lawrence, S., Rodriguez, J., He, Z., Cornejo, M.P., Mustafa, E.R., et al., 2020. Metabolic insights from a GHSR-A203E mutant mouse model. Molecular Metabolism 39:101004.

[35] Pantel, J., Legendre, M., Cabrol, S., Hilal, L., Hajaji, Y., Morisset, S., et al., 2006. Loss of constitutive activity of the growth hormone secretagogue receptor in familial short stature. Journal of Clinical Investigation 116(3):760—768.

[36] Zigman, J.M., Nakano, Y., Coppari, R., Balthasar, N., Marcus, J.N., Lee, C.E., et al., 2005. Mice lacking ghrelin receptors resist the development of diet-induced obesity. Journal of Clinical Investigation 115(12):3564—3572.

[37] Peris-Sampedro, F., Stoltenborg, I., Le May, M.V., Zigman, J.M., Adan, R.A.H., Dickson, S.L., 2021. Genetic deletion of the ghrelin receptor (GHSR) impairs growth and blunts endocrine response to fasting in Ghsr-IRES-Cre mice. Molecular Metabolism 51:101223.

[38] Scott, M.M., Perello, M., Chuang, J.C., Sakata, I., Gautron, L., Lee, C.E., et al., 2012. Hindbrain ghrelin receptor signaling is sufficient to maintain fasting glucose. PLoS One 7(8):e44089.

[39] Cabral, A., Valdivia, S., Fernandez, G., Reynaldo, M., Perello, M., 2014. Divergent neuronal circuitries underlying acute orexigenic effects of peripheral or central ghrelin: critical role of brain accessibility. Journal of Neuroendocrinology 26(8):542—554.

[40] Perello, M., Sakata, I., Birnbaum, S., Chuang, J.C., Osborne-Lawrence, S., Rovinsky, S.A., et al., 2010. Ghrelin increases the rewarding value of high-fat diet in an orexin-dependent manner. Biological Psychiatry 67(9):880—886.

[41] Fernandez, G., Cabral, A., Andreoli, M.F., Labarthe, A., M'Kadmi, C., Ramos, J.G., et al., 2018. Evidence supporting a role for constitutive ghrelin receptor signaling in fasting-induced hyperphagia in male mice. Endocrinology 159(2):1021—1034.

[42] Clegg, D.J., Brown, L.M., Zigman, J.M., Kemp, C.J., Strader, A.D., Benoit, S.C., et al., 2007. Estradiol-dependent decrease in the orexigenic potency of ghrelin in female rats. Diabetes 56(4):1051—1058.

[43] Frazao, R., Dungan Lemko, H.M., da Silva, R.P., Ratra, D.V., Lee, C.E., Williams, K.W., et al., 2014. Estradiol modulates Kiss1 neuronal response to ghrelin. American Journal of Physiology. Endocrinology and Metabolism 306(6):E606—E614.

[44] Davies, J.S., Kotokorpi, P., Eccles, S.R., Barnes, S.K., Tokarczuk, P.F., Allen, S.K., et al., 2009. Ghrelin induces abdominal obesity via GHS-R-dependent lipid retention. Molecular Endocrinology 23(6):914—924.

[45] Dallak, M.A., 2018. Acylated ghrelin induces but deacylated ghrelin prevents hepatic steatosis and insulin resistance in lean rats: effects on DAG/PKC/JNK pathway. Biomedicine & Pharmacotherapy 105:299—311.

[46] Li, Z., Xu, G., Qin, Y., Zhang, C., Tang, H., Yin, Y., et al., 2014. Ghrelin promotes hepatic lipogenesis by activation of mTOR-PPARgamma signaling pathway. Proceedings of the National Academy of Sciences of the United States of America 111(36):13163—13168.

[47] Zhang, S., Mao, Y., Fan, X., 2018. Inhibition of ghrelin o-acyltransferase attenuated lipotoxicity by inducing autophagy via AMPK-mTOR pathway. Drug Design, Development and Therapy 12:873—885.

[48] Abegg, K., Bernasconi, L., Hutter, M., Whiting, L., Pietra, C., Giuliano, C., et al., 2017. Ghrelin receptor inverse agonists as a novel therapeutic approach against obesity-related metabolic disease. Diabetes, Obesity and Metabolism 19(12):1740—1750.

[49] Guillory, B., Jawanmardi, N., Iakova, P., Anderson, B., Zang, P., Timchenko, N.A., et al., 2018. Ghrelin deletion protects against age-associated hepatic steatosis by downregulating the C/EBPalpha-p300/DGAT1 pathway. Aging Cell 17(1):e12688.

[50] Loch, D., Breer, H., Strotmann, J., 2015. Endocrine modulation of olfactory responsiveness: effects of the orexigenic hormone ghrelin. Chemical Senses 40(7):469—479.

[51] Ratcliff, M., Rees, D., McGrady, S., Buntwal, L., Hornsby, A.K.E., Bayliss, J., et al., 2019. Calorie restriction activates new adult born olfactory-bulb neurones in a ghrelin-dependent manner but acyl-ghrelin does not

enhance subventricular zone neurogenesis. Journal of Neuroendocrinology 31(7):e12755.

[52] Dickson, S.L., Luckman, S.M., 1997. Induction of c-fos messenger ribonucleic acid in neuropeptide Y and growth hormone (GH)-releasing factor neurons in the rat arcuate nucleus following systemic injection of the GH secretagogue, GH-releasing peptide-6. Endocrinology 138(2):771—777.

[53] Wu, C.S., Bongmba, O.Y.N., Lee, J.H., Tuchaai, E., Zhou, Y., Li, D.P., et al., 2019. Ghrelin receptor in agouti-related peptide neurones regulates metabolic adaptation to calorie restriction. Journal of Neuroendocrinology 31(7):e12763.

[54] Cabral, A., Fernandez, G., Tolosa, M.J., Rey Moggia, A., Calfa, G., De Francesco, P.N., et al., 2020. Fasting induces remodeling of the orexigenic projections from the arcuate nucleus to the hypothalamic paraventricular nucleus, in a growth hormone secretagogue receptor-dependent manner. Molecular Metabolism 32:69—84.

[55] Tong, J., Mannea, E., Aime, P., Pfluger, P.T., Yi, C.X., Castaneda, T.R., et al., 2011. Ghrelin enhances olfactory sensitivity and exploratory sniffing in rodents and humans. Journal of Neuroscience 31(15):5841—5846.

[56] Okuhara, Y., Kaiya, H., Teraoka, H., Kitazawa, T., 2018. Structural determination, distribution, and physiological actions of ghrelin in the Guinea pig. Peptides 99:70—81.

[57] Diano, S., Farr, S.A., Benoit, S.C., McNay, E.C., da Silva, I., Horvath, B., et al., 2006. Ghrelin controls hippocampal spine synapse density and memory performance. Nature Neuroscience 9(3):381—388.

[58] Rhea, E.M., Salameh, T.S., Gray, S., Niu, J., Banks, W.A., Tong, J., 2018. Ghrelin transport across the blood-brain barrier can occur independently of the growth hormone secretagogue receptor. Molecular Metabolism 18: 88—96.

[59] Perello, M., Cabral, A., Cornejo, M.P., De Francesco, P.N., Fernandez, G., Uriarte, M., 2019. Brain accessibility delineates the central effects of circulating ghrelin. Journal of Neuroendocrinology 31(7):e12677.

[60] Cabral, A., Fernandez, G., Perello, M., 2013. Analysis of brain nuclei accessible to ghrelin present in the cerebrospinal fluid. Neuroscience 253:406—415.